AD-A097 004 AEROSPACE CORP EL SEGUNDO CA GUIDANCE AND CONTROL DIV F/G 12/1
COLLISION HAZARD IN SPACE.(U)
FEB 81 V A CHOBOTOV F04701-80-C-0081
UNCLASSIFIED TR-0081(6790)-1 SD-TR-81-11 NL

1 OF 1
AD A
097004

END
DATE
FILMED
4-81
DTIC

REPORT SD-TR-81-11

LEVEL II

(12)

AD A097004

Collision Hazard in Space

V. A. CHOBOTOV
Guidance and Control Division
The Aerospace Corporation
El Segundo, CA 90245

25 February 1981

APPROVED FOR PUBLIC RELEASE;
DISTRIBUTION UNLIMITED

Prepared for

SPACE DIVISION
AIR FORCE SYSTEMS COMMAND
Los Angeles Air Force Station
P.O. Box 92960, Worldway Postal Center
Los Angeles, Calif. 90009

This final report was submitted by The Aerospace Corporation, El Segundo, CA 90245, under Contract F04701-80-C-0081 with the Space Division, PO Box 92960, Worldway Postal Center, Los Angeles, CA 90009. It was reviewed and approved for The Aerospace Corporation by L. J. Kulakowski, Engineering Group. Colonel D. F. Shane, Office of Plans (SD/CX), was the project engineer.

This report has been reviewed by the Public Affairs Office (SD/PAS) and is releasable to the National Technical Information Service (NTIS). At NTIS, it will be available to the general public, including foreign nations.

This technical report has been reviewed and is approved for publication. Publication of this report does not constitute Air Force approval of the report's findings or conclusions. It is published only for the exchange and stimulation of ideas.

Robert L. Dean, Lt Colonel, USAF
Director, Mission Planning

FOR THE COMMANDER

James P. Baker, Lt Colonel, USAF
Acting Assistant for Plans

UNCLASSIFIED

SECURITY CLASSIFICATION OF THIS PAGE (When Data Entered)

19

REPORT DOCUMENTATION PAGE

READ INSTRUCTIONS BEFORE COMPLETING FORM

1. REPORT NUMBER
18 SD-TR-81-11

2. GOVT ACCESSION NO.
AD-A097004

3. RECIPIENT'S CATALOG NUMBER

4. TITLE (and Subtitle)
6 COLLISION HAZARD IN SPACE.

5. TYPE OF REPORT & PERIOD COVERED
Final rept.

6. PERFORMING ORG. REPORT NUMBER
14 TR-0081(6790)-1

7. AUTHOR(s)
10 V. A. Chobotov

8. CONTRACT OR GRANT NUMBER(s)
15 F04701-80-C-0031

9. PERFORMING ORGANIZATION NAME AND ADDRESS
The Aerospace Corporation
El Segundo, CA 90245

10. PROGRAM ELEMENT, PROJECT, TASK AREA & WORK UNIT NUMBERS
11

11. CONTROLLING OFFICE NAME AND ADDRESS
Space Division
Air Force Systems Command
Los Angeles, Calif. 90009

12. REPORT DATE
25 Feb[redacted]981

13. NUMBER OF PAGES
65

14. MONITORING AGENCY NAME & ADDRESS(if different from Controlling Office)
12 | 67

15. SECURITY CLASS. (of this report)
Unclassified

15a. DECLASSIFICATION DOWNGRADING SCHEDULE

16. DISTRIBUTION STATEMENT (of this Report)

Approved for public release; distribution unlimited

17. DISTRIBUTION STATEMENT (of the abstract entered in Block 20, if different from Report)

18. SUPPLEMENTARY NOTES

19. KEY WORDS (Continue on reverse side if necessary and identify by block number)

Satellites
Collisions
Orbits
Space Debris Statistical Data
Operational and Design Policies

20. ABSTRACT (Continue on reverse side if necessary and identify by block number)

The statistical data on the known orbiting population of objects is presented and analyzed. Several methods for determining the probability of collision in orbit are described. Collision probabilities for low and geosynchronous orbits are evaluated. Potential operational and design policies for reducing the collision hazard and minimizing the proliferation of debris in space are examined.

PREFACE

The funding for this study was in part provided by the following program offices: Long Range Planning, Defense Support Systems, Plans and Systems Architecture - Satellite Position Management, Integration Directorate A and the Fleet Satellite Communications. The contributions of the following persons are also gratefully acknowledged: R. A. Marsh and R. J. Mercer for the data on the North American Air Defense Command geosynchronous and low altitude catalogs, K. H. Senechal, R. E. Simberg, and R. P. Gupta for aid in the numerical analyses, and H. K. Karrenberg for many helpful suggestions during the course of this study.

CONTENTS

PREFACE.......... 1

I. INTRODUCTION.......... 9

II. SPACE OBJECT POPULATION.......... 11

A. Growth Rate.......... 11

B. Origin and Distribution.......... 15

C. Density of Objects as a Function of Altitude.......... 17

1. Low Altitude Orbits.......... 17

2. Geosynchronous Orbits.......... 21

III. ANALYSIS AND RESULTS.......... 33

A. Uniform Density Method.......... 33

B. Variable Density Method.......... 37

C. Distance of Closest Approach Method.......... 45

1. General Considerations.......... 45

2. Miss Distance and Position Uncertainty.......... 45

IV. SUMMARY AND CONCLUSIONS.......... 59

APPENDIX. UNCLASSIFIED GEOSYNCHRONOUS CATALOG - ALPHABETICAL ORDER.......... 63

REFERENCES.......... 71

FIGURES

1. Cataloged Objects Population History.................................... 13

2. Computer View of a Sample of Space Objects........................... 14

3. Known Launches and Payload History.................................... 16

4. SKYNET 1B Geosynchronous Orbit Injection Geometry..................... 18

5. Cumulative Number of Objects vs. Geocentric Radius in Units of Earth Radius.. 19

6. Space Object Density vs. Altitude..................................... 20

7. Fraction of Objects vs. Orbital Parameters............................ 22

8. Fraction of Objects vs. Inclination................................... 23

9. Representative Satellite Trajectories Relative to Geopotential Geopotential Stable Points.. 24

10. NORAD Unclassified Geosynchronous Catalog............................ 25

11. Geostationary Communication Satellites............................... 26

12. Cumulative Number vs. Inclination for Geosynchronous Objects.......... 28

13. Cumulative Number vs. Eccentricity for Geosynchronous Objects......... 29

14. Object Density in Geosynchronous Orbits.............................. 30

15. Right Ascension of the Ascending Node in Geosynchronous Orbits........ 31

16. Toroidal Geometry for Geosynchronous Orbits.......................... 36

17. Probability of Collision - Low Earth Orbits (800 to 1500 km) for 1000 Days... 38

18. Probability of Collision - Geosynchronous Orbits for 1000 Days........ 39

19. Dwell Fraction vs. Latitude for Circular Orbits...................... 41

20. Collision Probability for Objects in Circular Geosynchronous Orbits in 1000 Days.. 43

21. Collision Probability for Objects in Eccentric Geosynchronous Orbits in 1000 Days.. 44

FIGURES (Continued)

22. Encounter Geometry for Mutually Inclined Circular Orbits.............. 46

23. Collision Probability as a Function of Position Uncertainty and Miss Distance (R_S = 20 ft).................................... 52

24. Collision Probability as a Function of Position Uncertainty and Miss Distance (R_S = 50 ft).................................... 53

25. Collision Probability as a Function of Position Uncertainty and Miss Distance (R_S = 50 ft) (Continued)........................... 54

26. Collision Probability as a Function of Position Uncertainty and Miss Distance (R_S = 100 ft)................................... 55

27. Collision Probability as a Function of Position Uncertainty and Miss Distance (R_S = 100 ft) (Continued).......................... 56

28. Maximum Collision Probability Per Pass (P_{max}) as Function of Effective Collision Radius to Miss Distance Ratio (R_S/R_{min}).. 57

29. WESTAR-A/OPS 6391 Collision Probability During the April 14 to April 23, 1980 Encounters in Geosynchronous Orbit.................... 58

30. Operational Procedures to Minimize Collision Hazard in Space.......... 62

TABLES

1. NORAD Catalog of all Objects for 27 April 1980........................ 12

2. Close Encounters Between OPS 6391 and WESTAR-A Geosynchronous Satellites.. 47

3. Summary of Present and Projected Collision Probabilities for a 1000-Day Mission... 60

PRECEDING PAGE BLANK-NOT FILMED

I. INTRODUCTION

Since 1957 the continuous use of space has resulted in the buildup of a large number of space objects such as active and spent payloads, rocket bodies, and miscellaneous debris, including numerous explosion fragments. A catalog of an estimated radar-trackable population of some 5000 satellites is maintained by the North American Air Defense Command (NORAD) and other agencies. These objects are a subset of an unknown but larger population of objects including those that are too small to be tracked by radar, but large enough to cause damage to another spacecraft by collision.

In view of this, much interest and concern have been expressed recently by several government agencies and international organizations regarding the orbiting debris problem and the associated collision hazard. Questions on the subject have been posed by the United Nations, NASA and the USAF/SD which have resulted in some assessments of the collision hazard at present and in the near future. Also, work is currently underway to revise the USAF/SD Regulation 550-11 to establish Space Division guidelines and responsibilities for program directors and offices involved in the management of geosynchronous satellites.

The purpose of the present study is to update the existing data on the orbiting population (Ref. 1), and to reexamine the collision hazard issues as currently perceived. Probabilities of collision at low altitudes and in the geosynchronous corridor will be estimated using approximate methods developed in the study. Potential operational and design approaches that can aid in reducing the space debris population growth rates will be outlined. It is hoped that these efforts will contribute towards a better understanding and awareness of the collision hazard so that appropriate action can be taken to maintain a relatively low risk environment for current and future satellite systems.

II. SPACE OBJECT POPULATION

A. GROWTH RATE

On the basis of a worldwide network of sensors, NORAD tracks and maintains a catalog of most of the manmade orbiting objects in space. Although NORAD is the primary source of orbit elements for these objects, other sources are NASA Satellite Situation Reports, RAE tables of earth satellites, TRW Space Log and various military and civilian agencies including those of the United Nations.

The orbiting population of objects consists of operational and decayed payloads, miscellaneous mission-related debris such as rocket bodies, clamps, shrouds, etc., and a multitude of explosion fragments. The latter constitute more than 60% of the trackable population (Ref. 2). For example, the number and type of objects listed in the NORAD catalog for 27 April 1980 are given in Table 1 (Ref. 3). It should be noted, however, that the cataloged population includes only those objects which can be tracked by radar (greater than 0.01 m^2 in area) up to 5000 km in altitude or optically. The currently estimated total population (down to 1 cm^2 in size) is believed to be on the order of 10,000 to 15,000 objects. In the geosynchronous corridor, the total population down to 1 cm^2 is probably as much as an order of magnitude greater than that which is cataloged. More detail on the synchronous satellite catalog is provided in the Appendix.

The approximate growth rate of the cataloged population is exhibited in Fig. 1. The observed rate of increase (on the basis of the smoothed data of Fig. 1) is between 9 and 13% per year depending on the time period of interest. An instructive computer illustration of the space objects which could be seen by an observer in a 300 nmi circular orbit for a period of 10 seconds is displayed in Fig. 2 where the apparent size of the object (circle radius) denotes relative distance from the observer.

Table 1. NORAD Catalog of All Objects for 27 April 80

Earth Orbit Payloads		1055	
Earth Orbit Debris		3384	
Deep Space Payloads		61	
Deep Space Debris		52	
	Current Objects	4552	4552
Decayed Payloads		1399	
Decayed Debris		5831	
	Decayed Objects	7230	7230
Total Objects			11782

Synchronous Population - 28 April 80

Satellites		
DOD(SCF)/NATO	23	
NASA	17	
COMSAT CORP	13	
LINCOLN LABS, RCA, W.U., ESA	10	
USSR	16	
UK, CAN, JAP, FR, IT, INDONESIA	18	
	97	97
Rocket Bodies and Old Satellites		
With Current Tracking	47	
No Recent Tracking	56	
	103	103
Total Synchronous		200

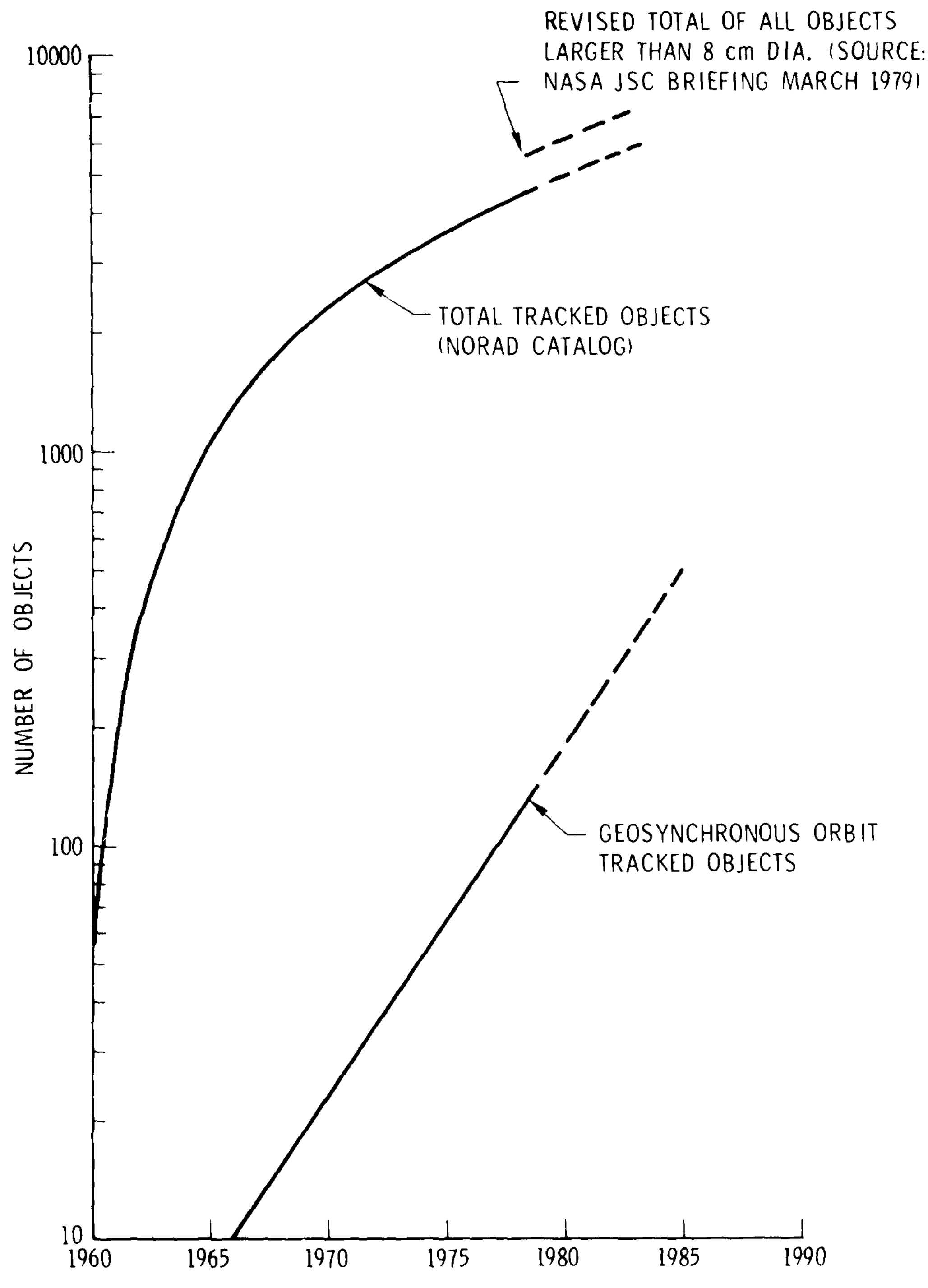

Fig. 1. Cataloged Objects Population History

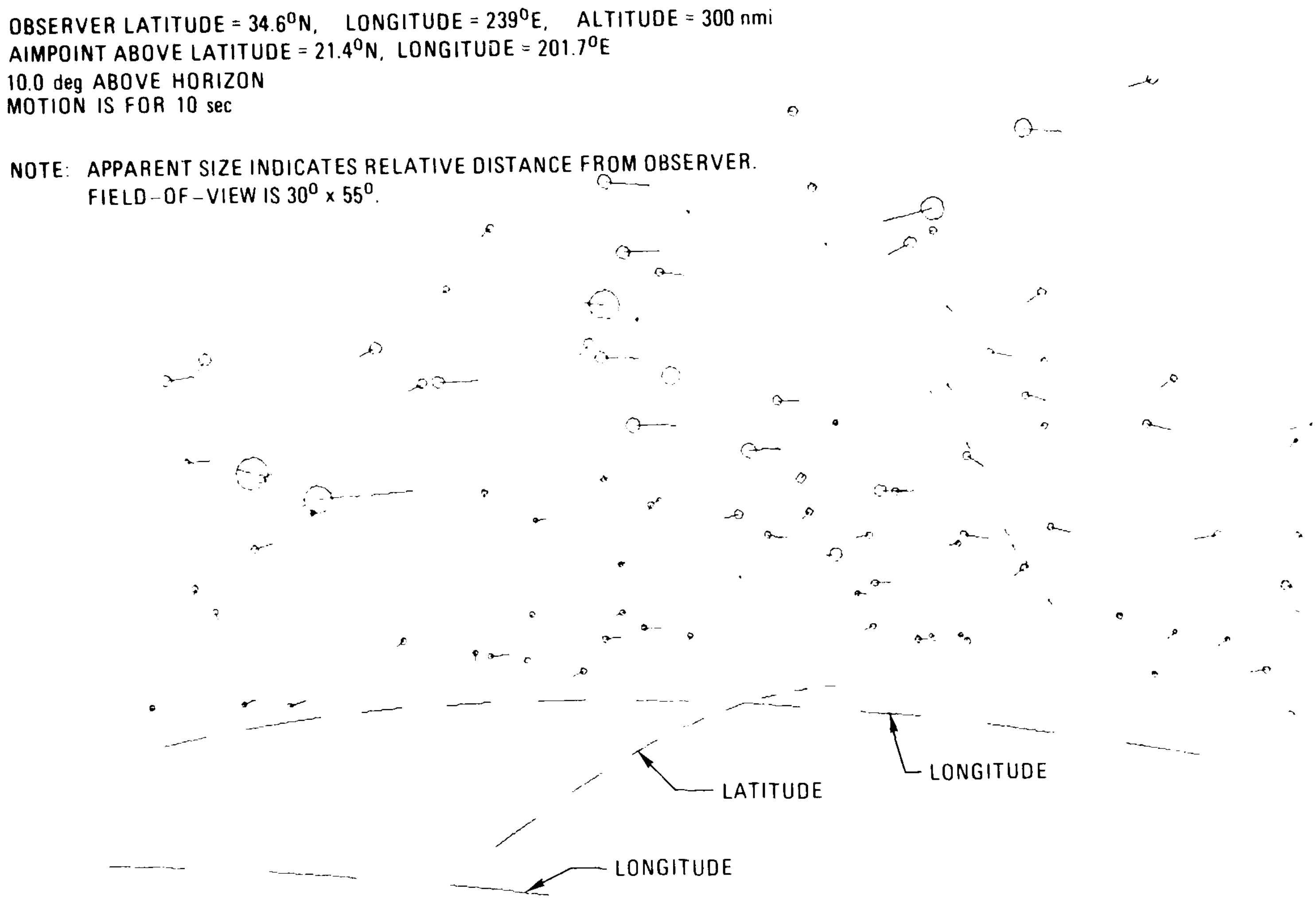

Fig. 2. Computer View of a Sample of Space Objects in a 300 nmi Circular Orbit

B. ORIGIN AND DISTRIBUTION

The principal sources of the orbiting population of objects to date have been the nearly 2000 launches by the U.S., the USSR, and several other countries. The history of known launches and payloads placed in orbit since 1975 is exhibited in Fig. 3. The principal U.S. launch vehicles are the Delta, Atlas/Agena, Centaur, Titan III and the Scout stages which have accounted for the estimated 33 U.S. launches in 1978. The total of 87 USSR launches in 1978 have resulted in a large number of the COSMOS series of satellites some of which were returned to earth or commanded into a destructive reentry into the atmosphere. By 1 January 1979 there were six launches by France, four by Japan, two by China and one by the U.K. From 1968 the yearly total number of launches varied between 106 and 128 for all countries (Ref. 4).

Payload and rocket body explosions in orbit are another source of space debris. It is known for example, that there have been over 50 such explosions as of 4 October 1978. A number of spacecraft explosions are known to have taken place in orbit related to antisatellite tests (ASATs) and/or attempts to inject payloads into geosynchronous orbit. A recent example of the latter was the apparent loss of the RCA Satcom 3 and the Japanese ECS 2 satellites which seem to have experienced anomalous burns of the apogee injection motors that resulted in a loss of telemetry before the completion of the insertion burn. Another example of such a malfunction is the SKYNET 1B launch on 19 August 1970 on a Thor-Delta vehicle which placed a communication payload into a 137 × 20099 nmi transfer orbit. On 22 August 1970, the apogee burn motor (ABM) was fired which should have placed the satellite into a nearly synchronous equatorial orbit. Approximately 14 seconds after the initiation of the apogee burn, all tracking and telemetry data were abruptly lost. Subsequent analyses of the data (Refs. 5 and 6) indicated that the ABM performed anomalously resulting in "regressive burning." An estimated ΔV = 4000 fps out of the required ΔV = 5814 fps appears to have been added at apogee. The resultant orbit for the assumed explosion fragments was estimated as approximately 5192 × 20088 nmi inclined 5.30° to the equator. The velocity at apogee relative to the geosynchronous velocity is about 1700 fps which may represent

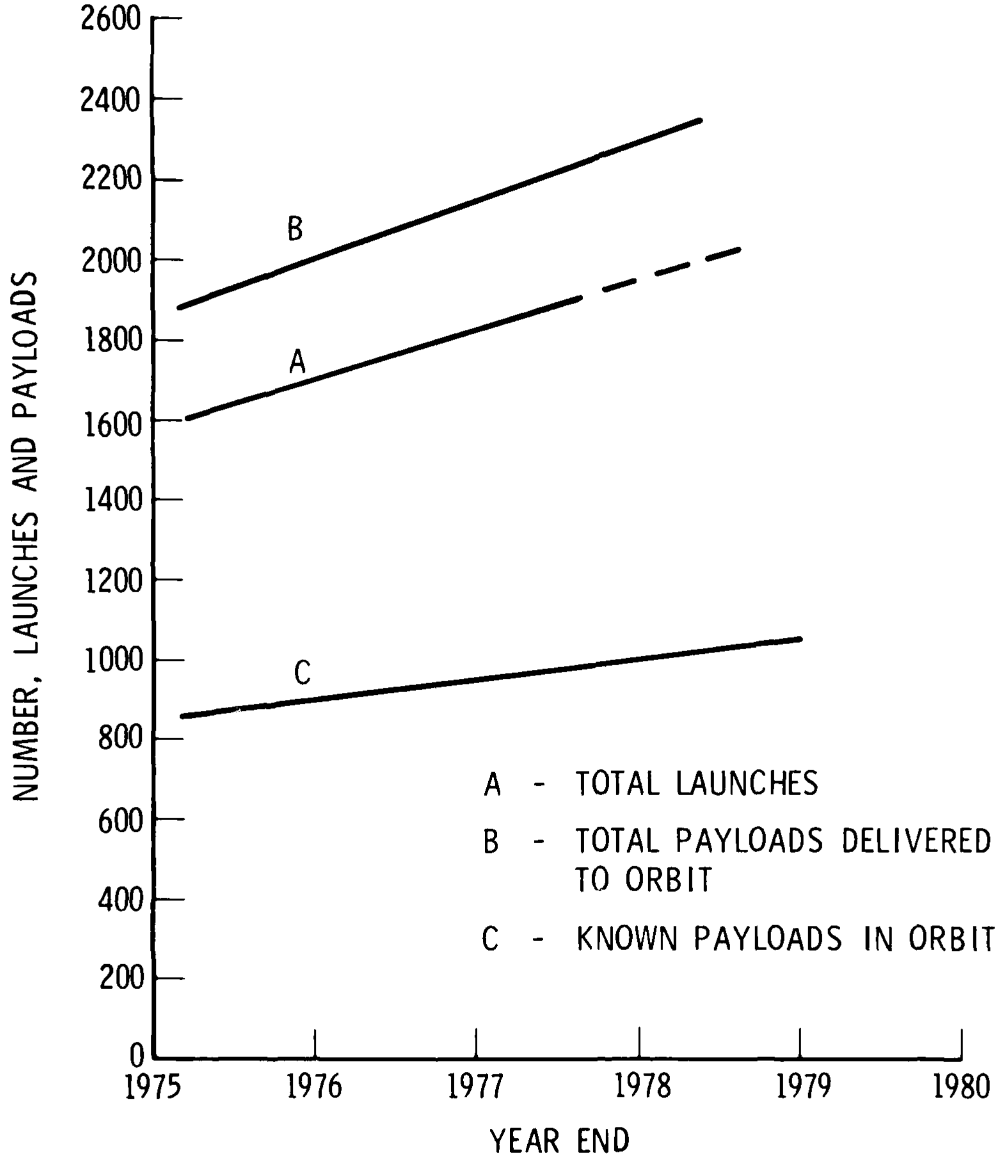

Fig. 3. Known Launches and Payload History

a significant collision hazard to any geosynchronous object in the vicinity of this orbit. The number and distribution of the explosion fragments, if an explosion in fact occurred, cannot be easily determined. However, the high perigee altitude of the final orbit precludes any significant reduction of the debris because of atmospheric or other perturbative effects. Figure 4 exhibits the orbit geometry for this event.

Other potential sources of space debris are collisions between debris objects and spacecraft or other debris objects. It is considered likely, for example, that the solar panel malfunction on the geosynchronous GEOS-2 spacecraft is a result of a collision with a small object (Ref. 7). Also, the breakup of PAGEOS balloon in July, 1975 after 9 years in orbit appears to have resulted from a similar cause. The low orbit COSMOS 954 was similarly reported to have suffered a sudden depressurization thought to be caused by a collision with debris (Ref. 2). Air Force satellite programs in synchronous orbit have reported, on two separate occasions, sudden small changes in spacecraft angular momentum. These unexplained changes may have been caused by impacts with natural or manmade objects.

The possibility of a self-perpetuating debris belt caused by intercollisions between objects in space also exists. This process would parallel certain theories concerning the growth of the asteroid belt. The debris flux in such a belt could exceed the natural meteoroid flux in the not too distant future if present trends continue (Ref. 8).

C. DENSITY OF OBJECTS AS A FUNCTION OF ALTITUDE

1. LOW ALTITUDE ORBITS

A total of 4174 space objects from the NORAD Catalog for April 28, 1980 have been examined numerically to determine the distribution with altitude. The results are presented in Figs. 5 and 6. It can be seen that the majority of satellites are within 1.5 earth radii (E.R.) with a small increase to synchronous altitude where an increment occurs at 6.62 E.R. Figure 6 indicates that the greatest density of objects occurs between 500 and 1500 km altitude. Distributions by semimajor axis A (normalized with respect to earth

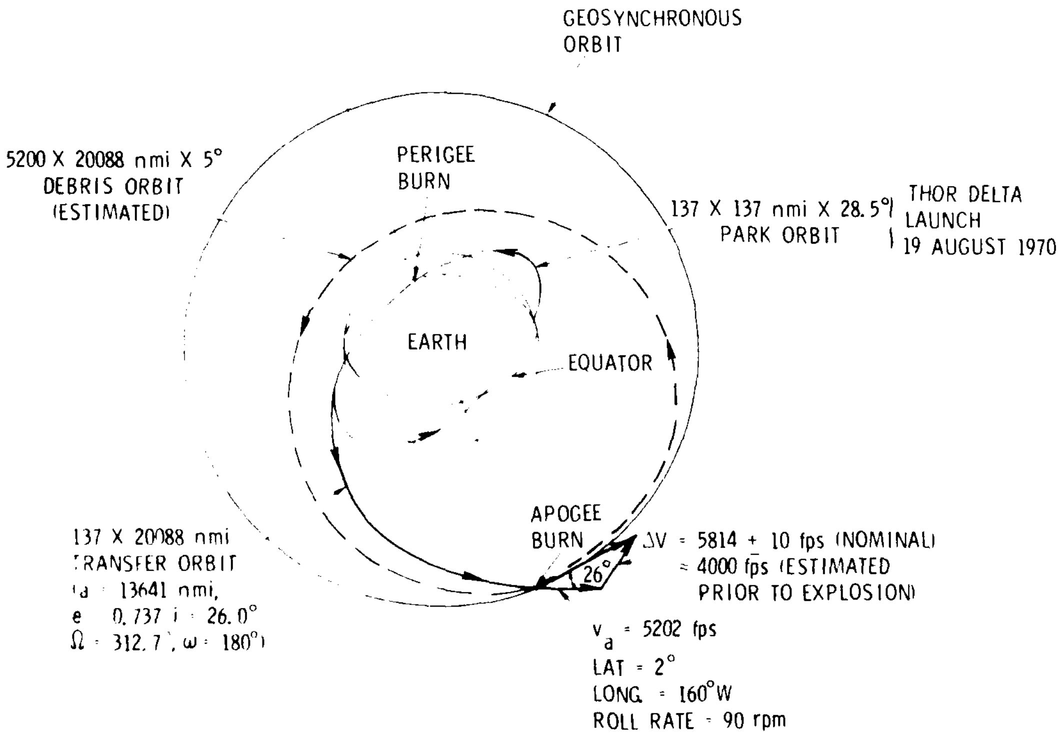

Fig. 4. SKYNET 1B Geosynchronous Orbit Injection Geometry

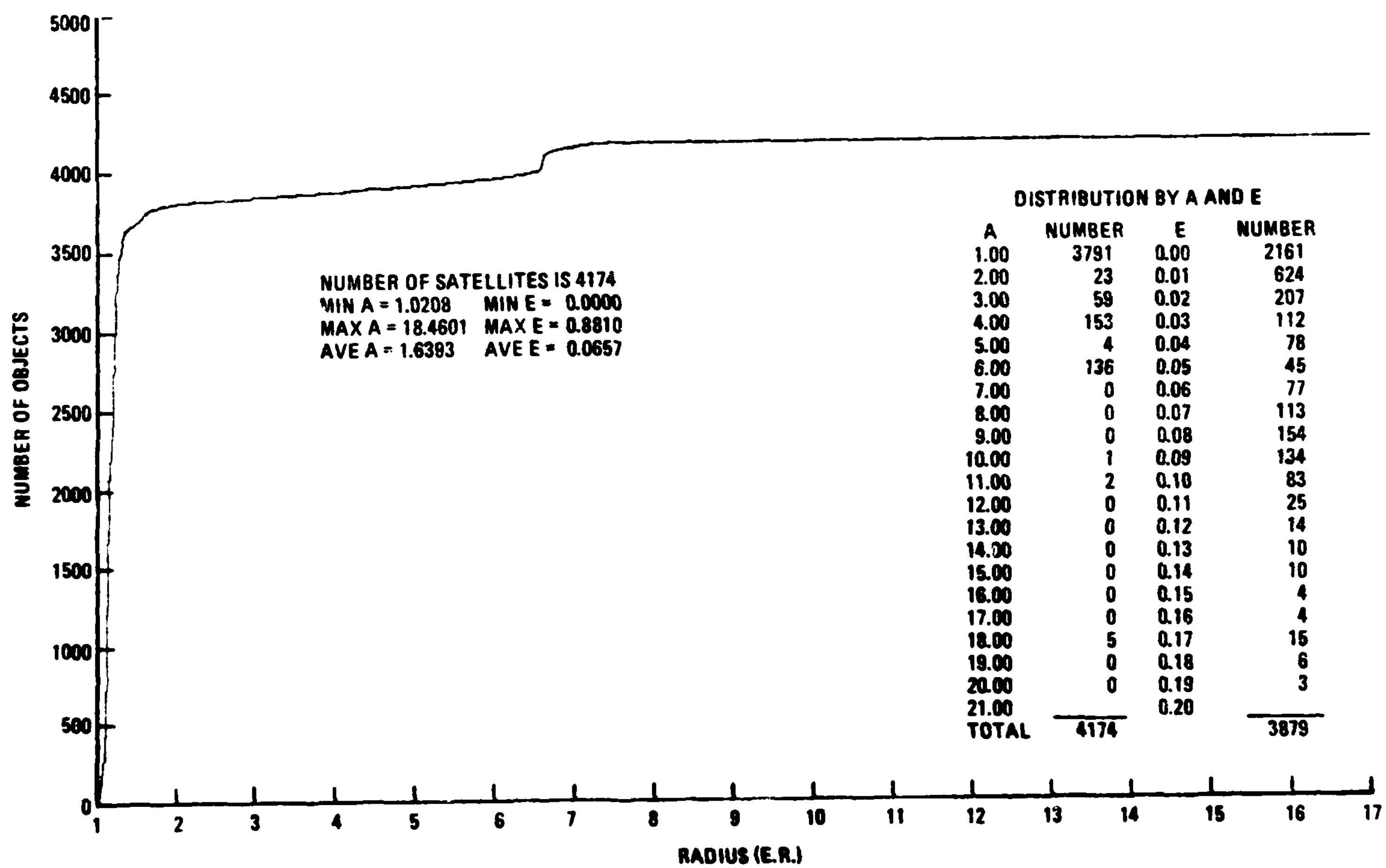

A	NUMBER	E	NUMBER
1.00	3791	0.00	2161
2.00	23	0.01	624
3.00	59	0.02	207
4.00	153	0.03	112
5.00	4	0.04	78
6.00	136	0.05	45
7.00	0	0.06	77
8.00	0	0.07	113
9.00	0	0.08	154
10.00	1	0.09	134
11.00	2	0.10	83
12.00	0	0.11	25
13.00	0	0.12	14
14.00	0	0.13	10
15.00	0	0.14	10
16.00	0	0.15	4
17.00	0	0.16	4
18.00	5	0.17	15
19.00	0	0.18	6
20.00	0	0.19	3
21.00		0.20	
TOTAL	4174		3879

Fig. 5. Cumulative Number of Objects vs. Geocentric Radius in Units of Earth Radius

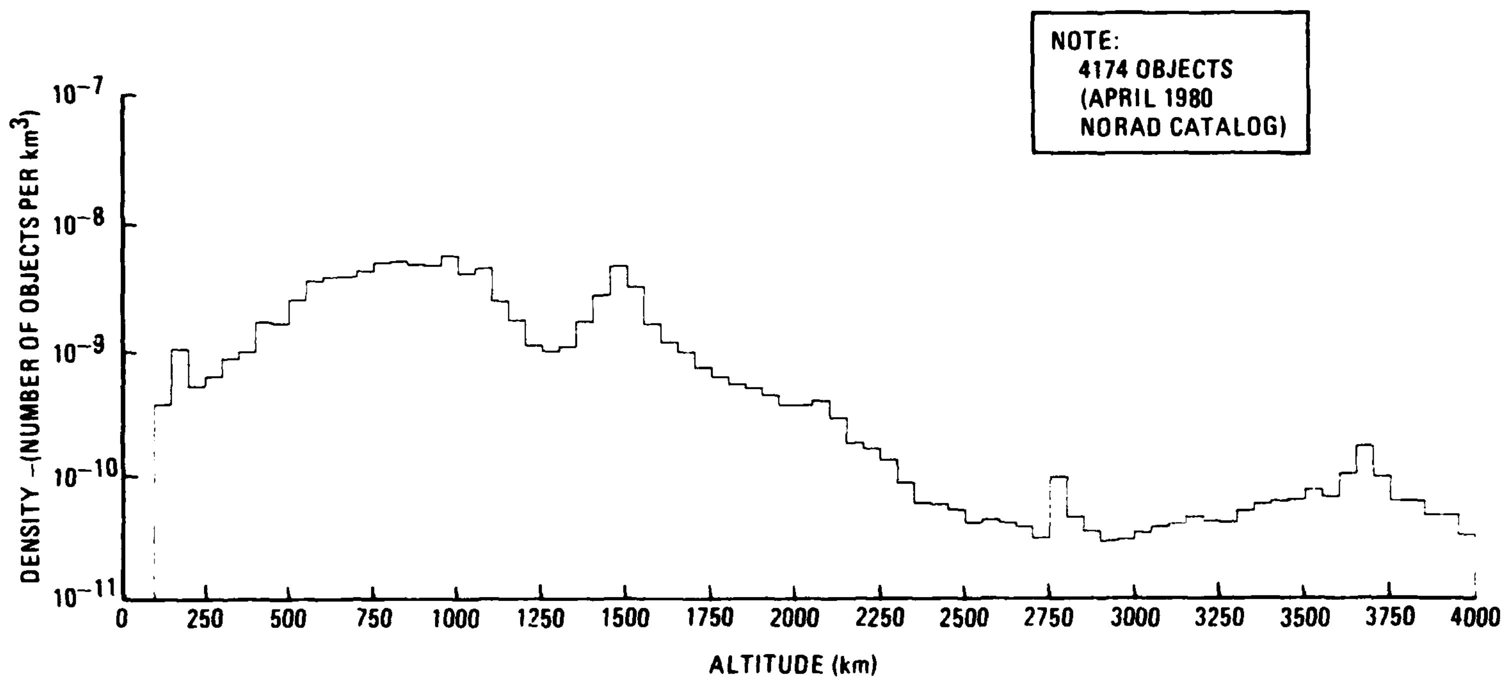

Fig. 6. Space Object Density vs. Altitude

radius), eccentricity E, ascending node (NODE) and the argument of perigee (OMEGA) are given in Fig. 7. It can be seen, for example, that there are 3791 objects with A greater than 1 but less than 2, and E greater than zero but less than 0.01. The distribution with respect to orbital inclination (INC) is given in Fig. 8.

2. GEOSYNCHRONOUS ORBITS

The geosynchronous region of space is a unique corridor where most of the present and future communication satellites are or will be located. The principal reason for this is that these satellites appear to be either stationary with respect to the earth or are slowly drifting relative to some initial longitude. The satellites are stationary when they are in circular orbits in the equatorial plane with periods of revolution equal to the rotational period of the earth. Secular or continuous drifting occurs due to slight differences in the orbital periods of revolution. Periodic drifting may also occur because of orbital eccentricity or inclination effects as well as perturbing effects of the geopotential field. For example, the $J_{2,2}$ tesseral harmonic causes an oscillatory (librational) motion about the geopotential stable points at 75.3°E and 255.3°E longitudes with long periods (on the order of years) of libration (see Fig. 9). A large number of objects librating about these points may pose an additional hazard to the active payloads placed at or near these locations. The longitudinal location for 154 geosynchronous objects listed in the appendix is illustrated in Fig. 10. NORAD publishes the orbital elements on these objects on the basis of data obtained from NORAD, the Satellite Control Facility (SCF), NASA and Intelsat tracking networks. The data on the orbital elements is provided by NORAD in the form of punched cards received via TWX on a daily basis. Updates for any given object are provided typically within a one or two week period.

Figure 11 presents the longitudinal location of the current and planned communication satellites in geosynchronous orbit (Refs. 9 to 11). Many of these comsats are station-kept within small longitudinal and latitude bands while others drift as the result of natural forces. A few have also been removed from geosynchronous orbit after the completion of their mission (e.g.,

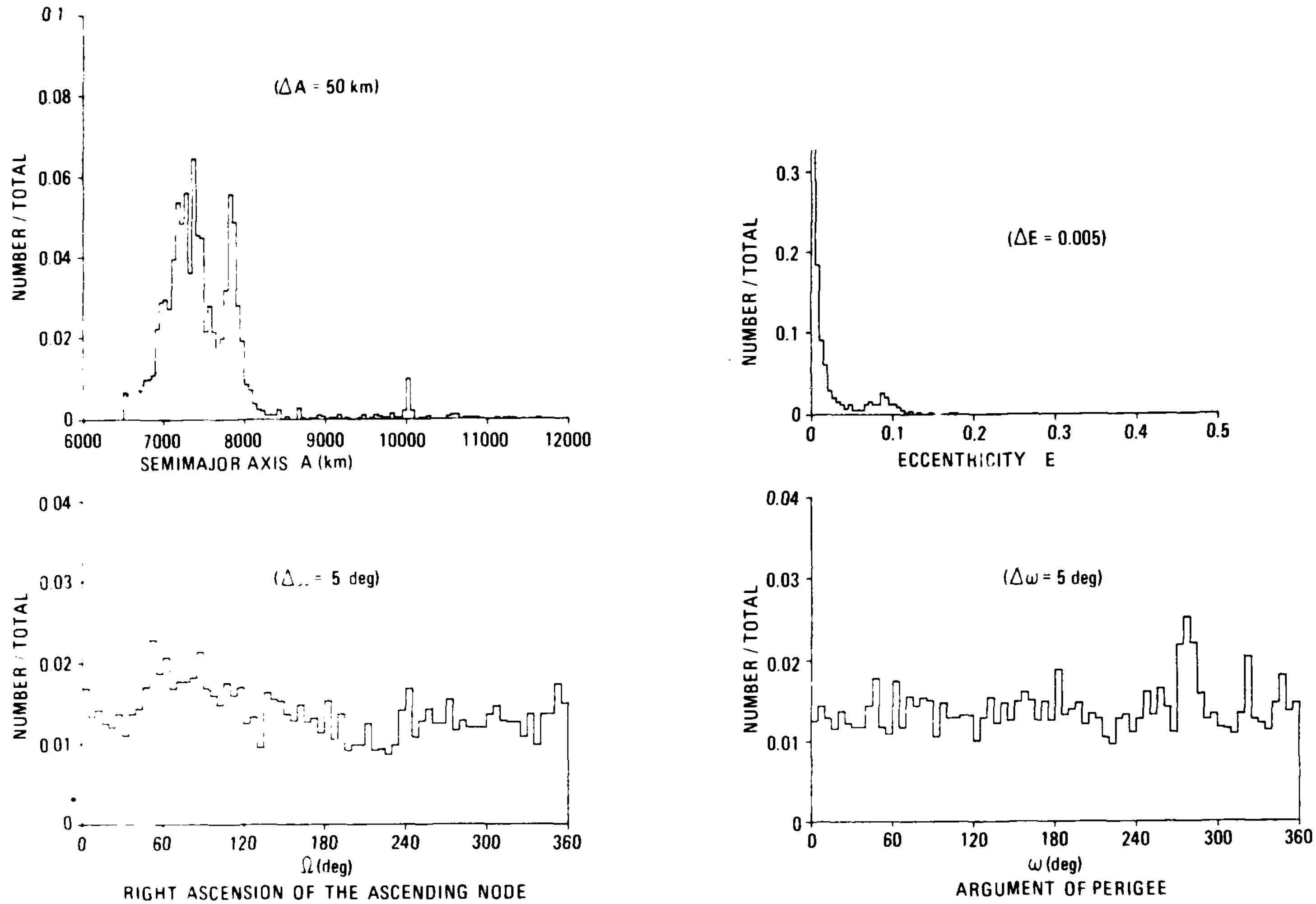

Fig. 7. Fraction of Objects vs. Orbital Parameters

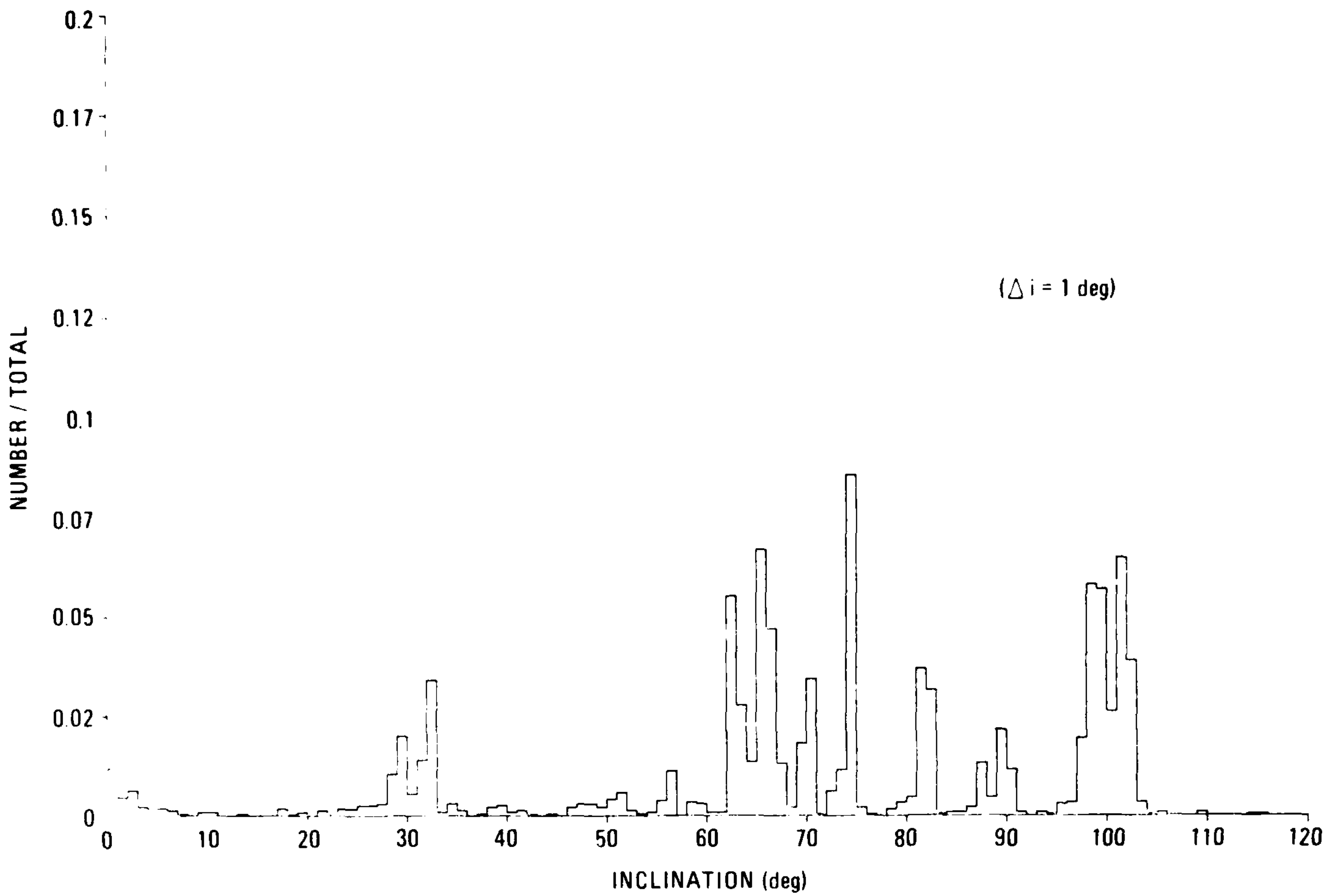

Fig. 8. Fraction of Objects vs. Inclination

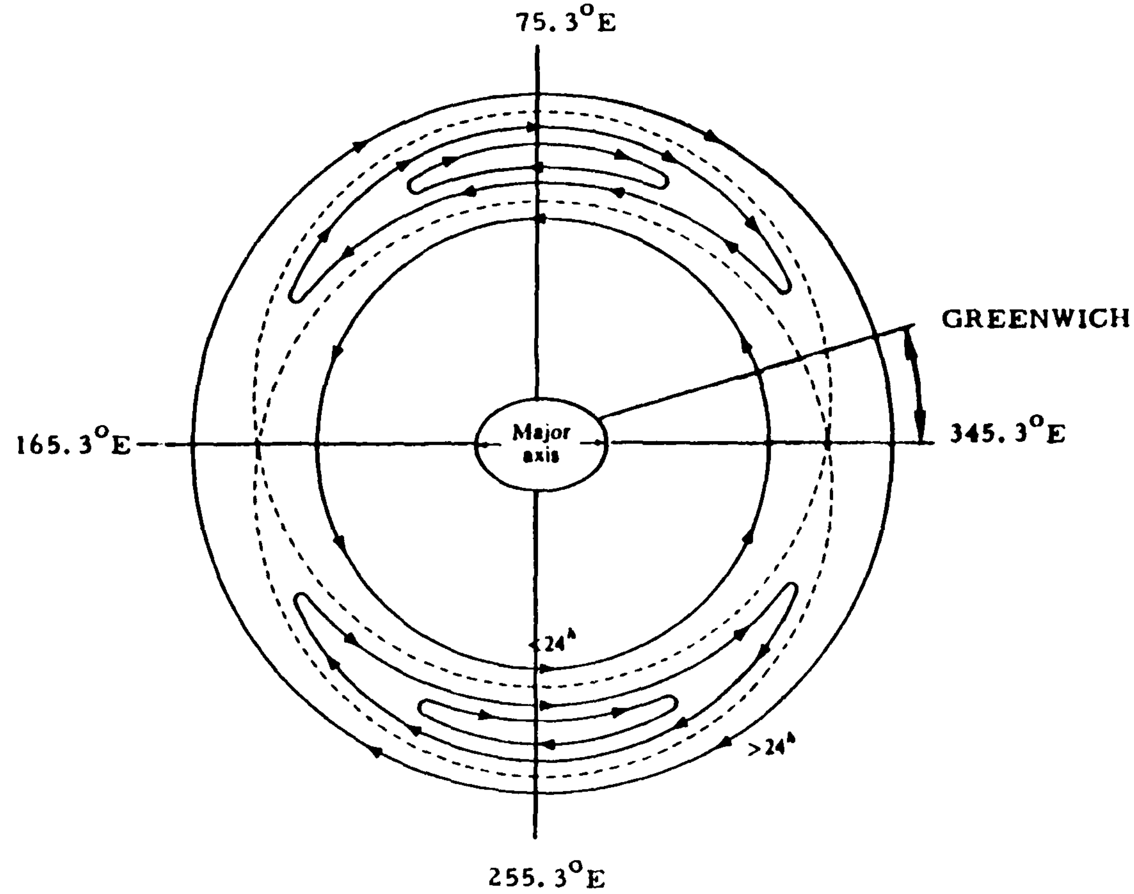

Fig. 9. Representative Satellite Trajectories Relative to Geopotential Stable Points

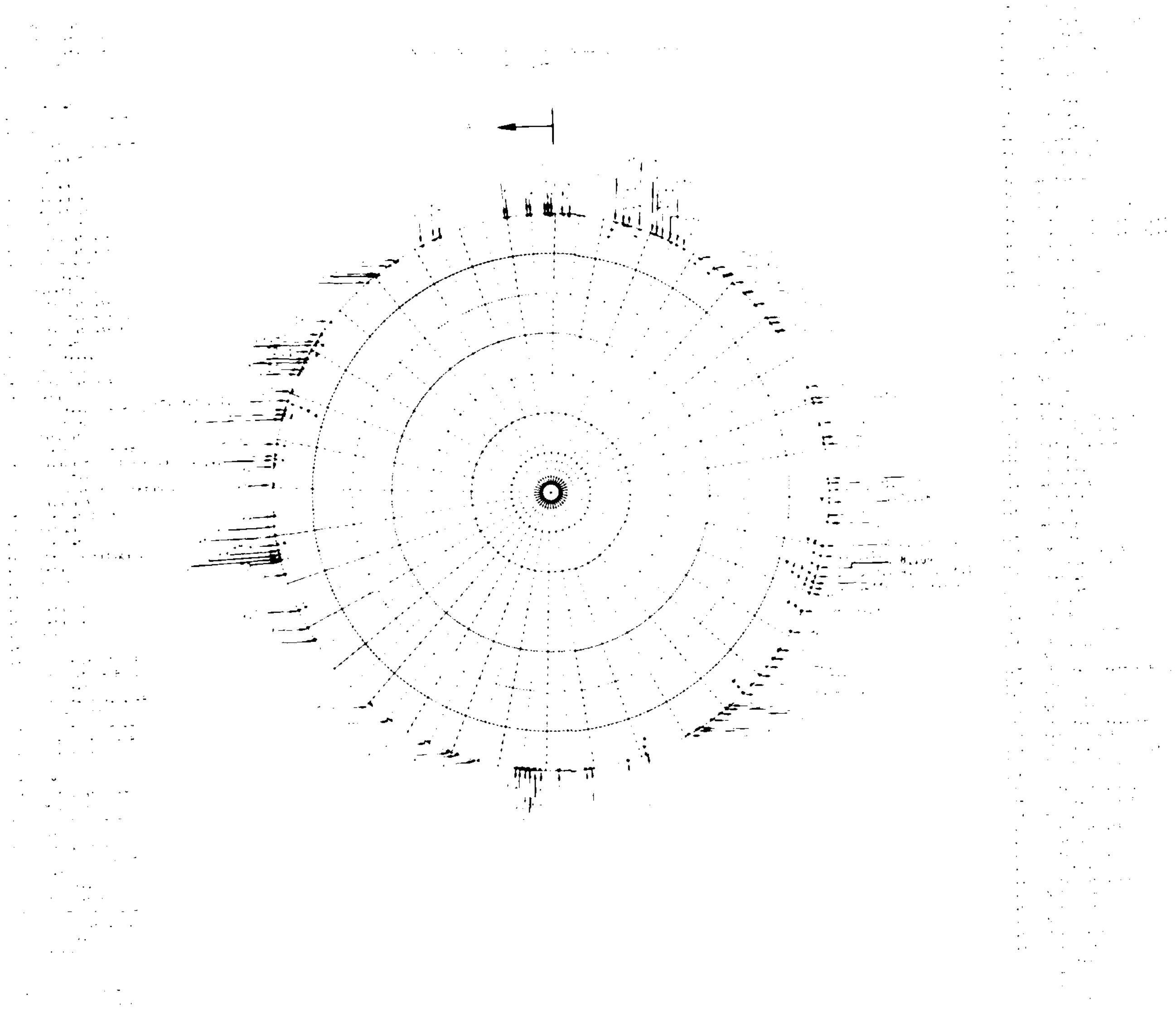

Fig. 10. NORAD Unclassified Geosynchronous Catalog

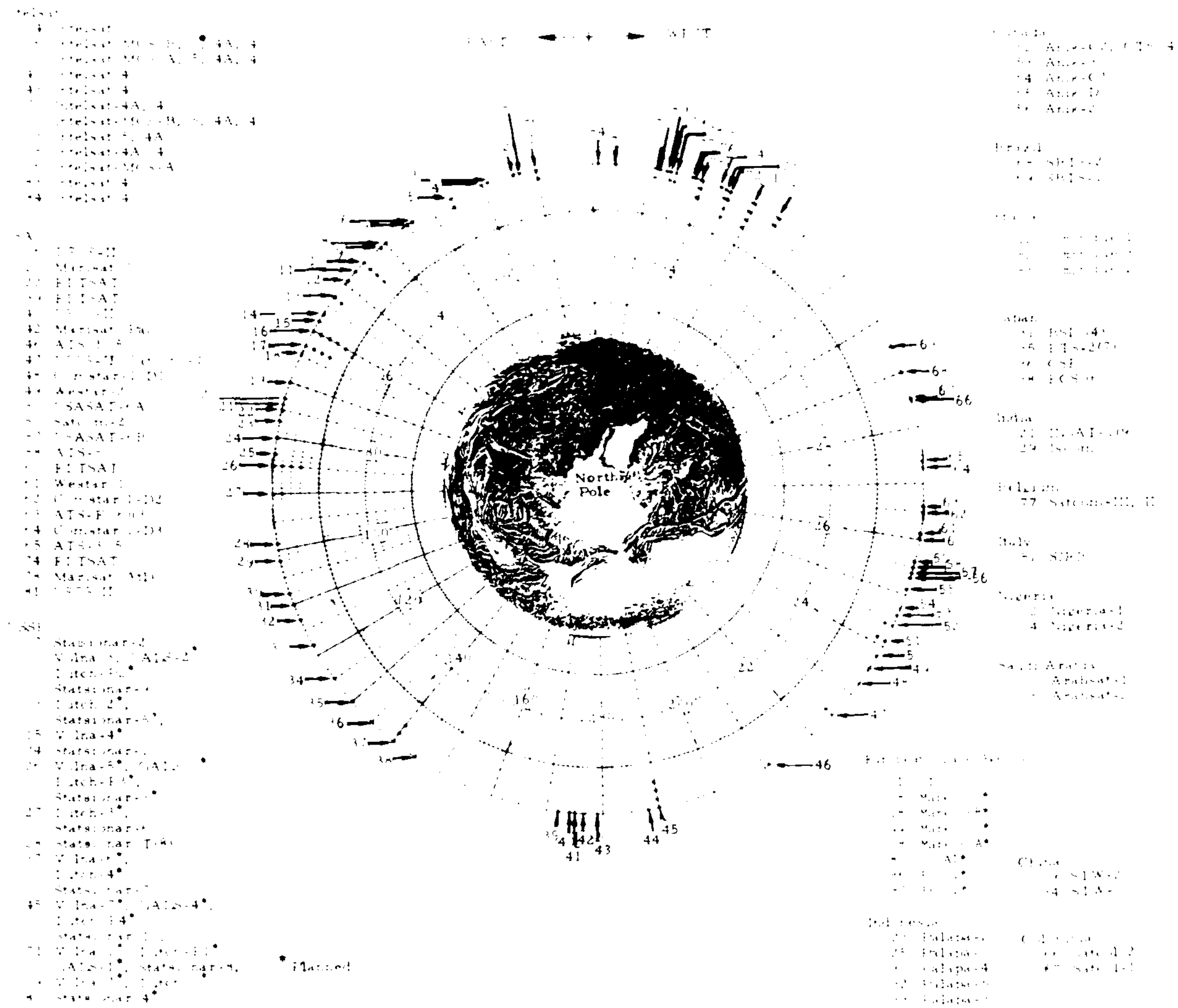

Fig. 11. Geostationary Communication Satellites

Intelsat 3, F-2, F-4 and F-6 to altitudes of 400 to 3700 km above synchronous altitude)(Ref. 12). The ATS-F has been removed from the synchronous altitude orbit to an altitude 250 nmi below synchronous. The distribution of a sample of 134 geosynchronous objects with inclination and eccentricity is given in Figs. 12 and 13, respectively. These results indicate that typical geo-synchronous orbits are nearly circular with low inclinations relative to the equator. A few satellites (e.g. ELECTRON, and their rocket bodies have inclinations above 60° (see Appendix). Object density, illustrated in Fig. 14, decreases as the altitude from the geosynchronous orbit and latitude increase. The results in Fig. 14 were obtained numerically by taking "snapshots" of objects once each hour over a period of twenty-four hours within a torus of latitude band $\Delta\phi$ and altitude band Δh centered about the geosynchronous altitude. The total number of observations was then summed and divided by 24 to get an average number of sightings in each band. The average density is the number of sightings divided by the volume of the torus. The nonuniformity of the inclinations of the objects orbits within each latitude band is illustrated in Fig. 14 by the average inclination $\bar{i}$ as noted.

The ascending node distribution for 154 geosynchronous objects presented in Fig. 15 indicates that the orbital planes are not distributed uniformly, but tend to be concentrated in certain regions of space. The impact of this is to increase the probability of collision for some satellites above the representative figures calculated for the synchronous class of satellites.

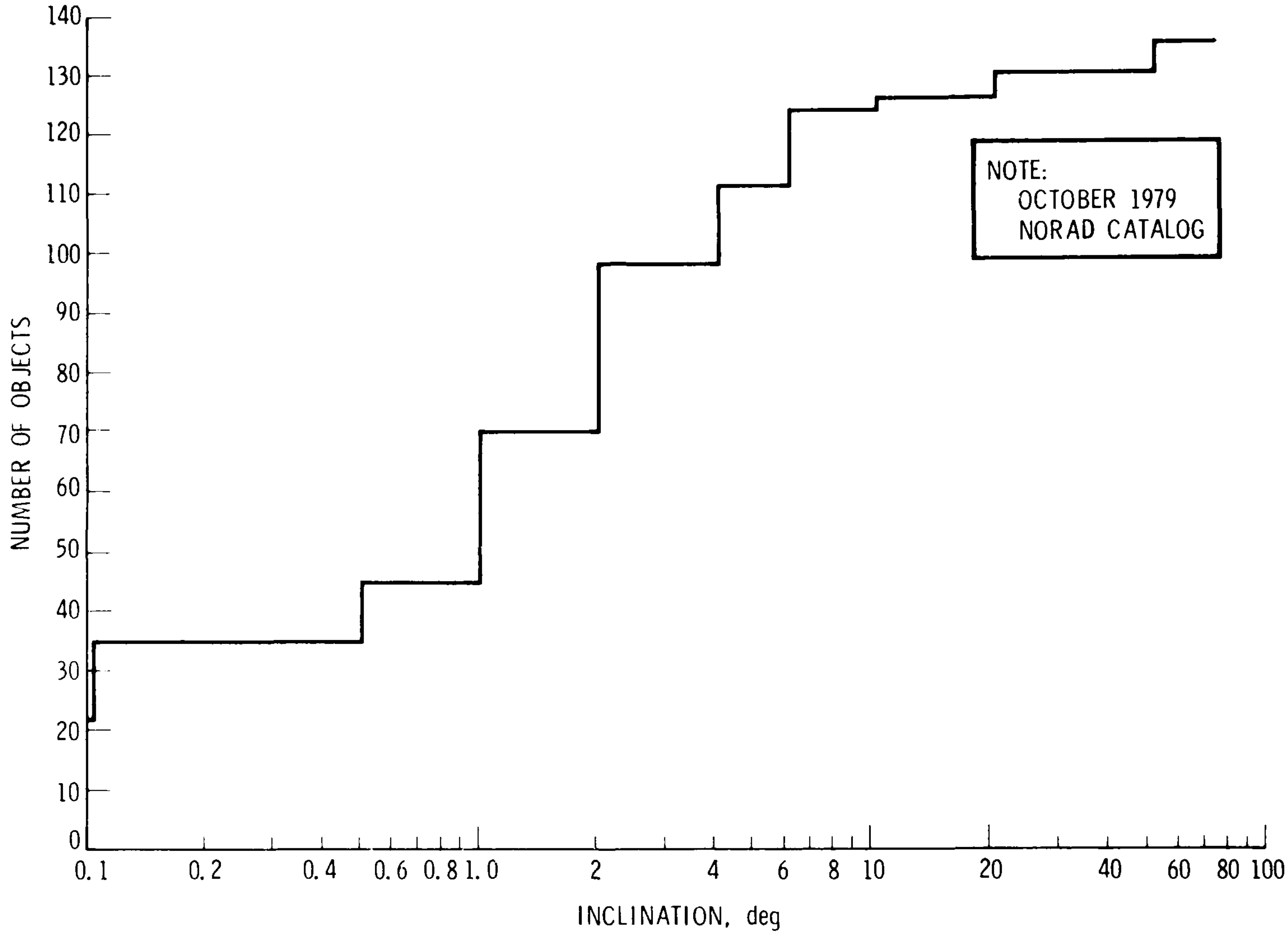

Fig. 12. Cumulative Number vs. Inclination for Geosynchronous Objects

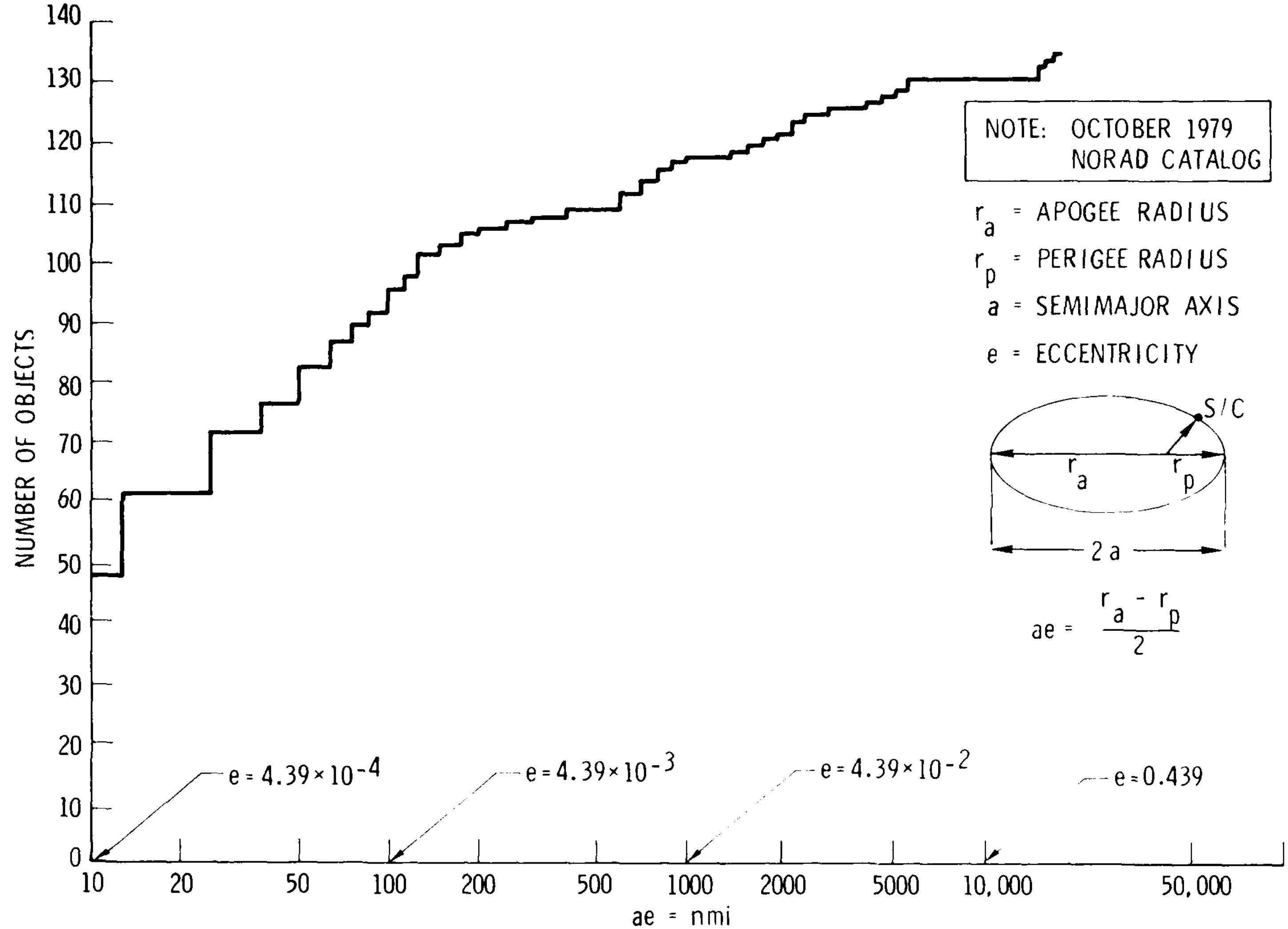

Fig. 13. Cumulative Number vs. Eccentricity for Geosynchronous Objects

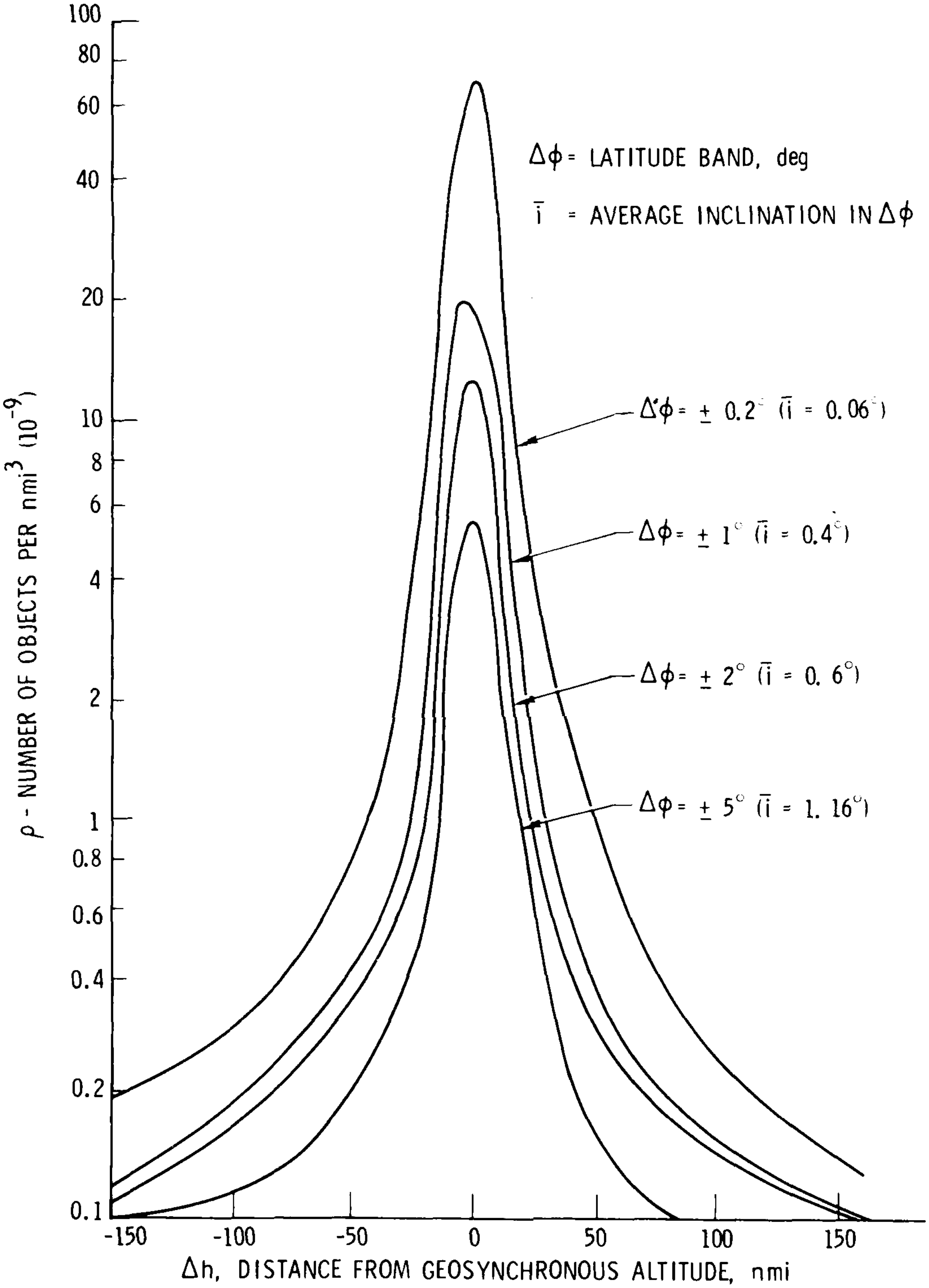

Fig. 14. Object Density in Geosynchronous Orbits

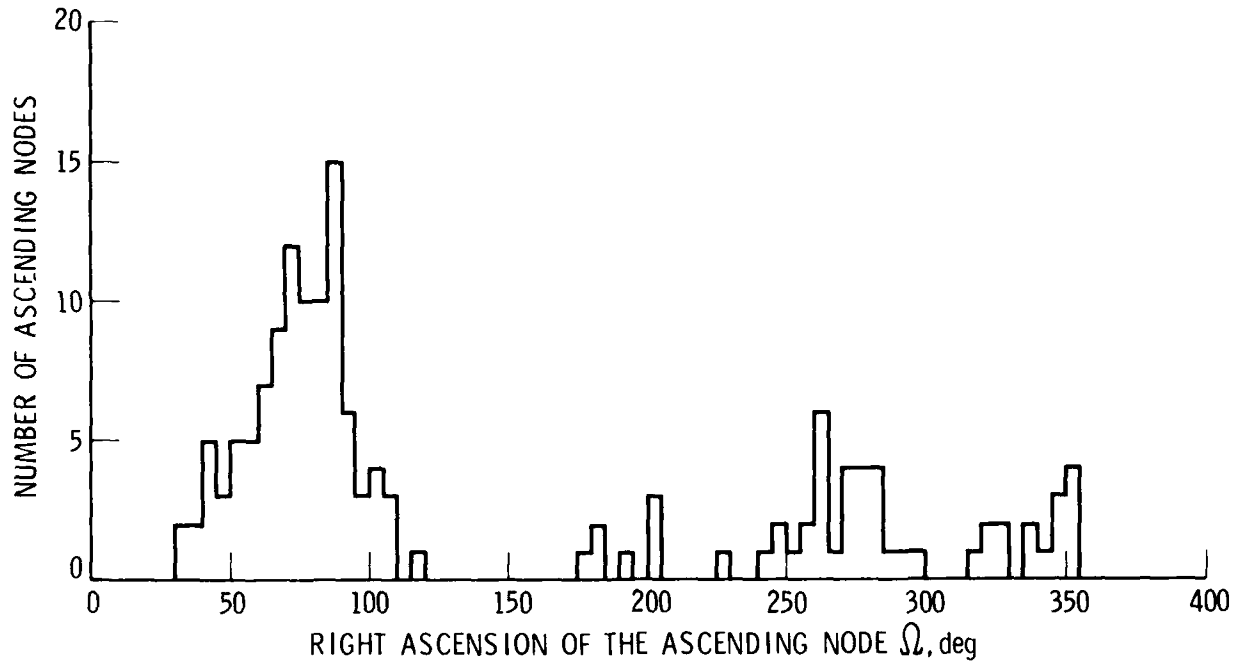

Fig. 15. Right Ascension of the Ascending Node in Geosynchronous Orbits

III. ANALYSIS AND RESULTS

A. UNIFORM DENSITY METHOD

The probability that any two satellites will collide is generally a function of their orbital parameters, size and time. The collision cannot take place until the orbits intersect or approach each other to within the dimensions of the satellites of interest. This may occur even for initially nonintersecting orbits because of the effects of the earth's oblateness, air drag and solar-lunar perturbations which alter the orbital parameters in time.

An approximate, yet reasonably accurate method for estimating the probability of collision between a target satellite of projected area A_c and a debris object is based on the assumption that the space object density ρ is uniform (constant) and that the target area A_c sweeps out a volume $A_c\Delta t$ in time Δt. It can be shown (Ref. 1) that the fractional number of objects encountered in the volume $A_c\ \Delta t$ is then equal to the probability of collision if it is much less than unity. Thus,

$$p(\mathrm{col}) = \rho v_r A_c \Delta t \tag{1}$$

where v_r is the average relative velocity between the satellite and the set of objects considered. For example, $v_r \approx 7$ km/sec for circular orbits up to 2000 km in altitude (Ref. 8).

The relative velocity v_r at the trace intersection between any two satellites in orbit planes with a mutual inclination of Δi can be expressed as (Ref. 1):

$$v_r = \sqrt{\frac{\mu}{r_x}}\left\{4 - \left(\frac{1}{A_1} + \frac{1}{A_2}\right) - 2\sqrt{\left[2 - \frac{1}{A_1} - A_1\left(1 - e_1^2\right)\right]\left[2 - \frac{1}{A_2} - A_2\left(1 - e_2^2\right)\right]} - 2\sqrt{A_1\left(1 - e_1^2\right)A_2\left(1 - e_2^2\right)}\cos\Delta i\right\}^{1/2} \tag{2}$$

where r_x is the radius at trace intersection and $A_1 = a_1/r_x$, $A_2 = a_2/r_x$. Here a_1, a_2, e_1, e_2, μ are the semimajor axes, eccentricities and the gravitational constant, respectively.

For the case of a circular and an eccentric orbit (e.g. $e_2 = 0$, $r_x = a_2$) Eq. (2) becomes

$$v_r = \sqrt{\frac{\mu}{r_x}} \left[3 - \frac{1}{A_1} - 2\sqrt{A_1\left(1 - e_1^2\right)} \cos \Delta i\right]^{1/2} \tag{3}$$

For circular orbits of equal period (i.e., $a_1 = a_2$, $e_1 = e_2 = 0$), Eq. (2) reduces to

$$\begin{aligned} v_{rc} &= 2v_c \sin \frac{\Delta i}{2} \\ &\approx v_c \sin \Delta i \qquad \text{for } \Delta i \text{ small.} \end{aligned} \tag{4}$$

which is equal approximately to the cross-track (normal) component of relative velocity at encounter with v_c = circular orbital velocity. An average relative velocity $\bar{v}_{rc}$ for this case can be defined as an average value of v_{rc} over a mean anomaly range $-\pi/2 < M < \pi/2$, i.e.

$$\begin{aligned} \bar{v}_{rc} &\approx \frac{v_c}{\pi} \sin \Delta i \int_{-\pi/2}^{\pi/2} \cos M dM \\ &\approx \frac{2v_c}{\pi} \sin \Delta i \end{aligned} \tag{5}$$

An approach which can be applied to the case of a spacecraft in a circular, inclined orbit is based on the determination of object density in a spheroidal torus containing the spacecraft orbit (Fig. 16). This approach is similar to that used in the theory of interplanetary encounters (Ref. 13). The spheroidal torus is defined by the relative orbit plane inclination Δi and the spacecraft orbit radius R. The probability of the object colliding with the spacecraft in a time interval Δt is

$$p(col/\Delta t) = 1 - e^{-\lambda \Delta t} \approx \lambda \Delta t \qquad \text{for } \lambda \Delta t \ll 1 \tag{6}$$

where

$$\lambda = \rho v_r A_c = \frac{S^2 v_r}{2\, T\, |u_r| \sin \Delta i}$$

= impact rate per unit time

T = object orbit period of revolution

S = R_s/R

R_s = spacecraft radius

v_r = relative velocity at encounter

$|u_r|$ = absolute value of the radial component of v_r

For a circular target orbit and an eccentric object orbit (Refs. 1, 13)

$$\frac{v_r}{|u_r|} = \left[\frac{3 - \frac{1}{A_1} - 2\sqrt{A_1(1 - e_1^2)} \cos \Delta i}{2 - \frac{1}{A_1} - A_1(1 - e_1^2)} \right]^{1/2} \tag{7}$$

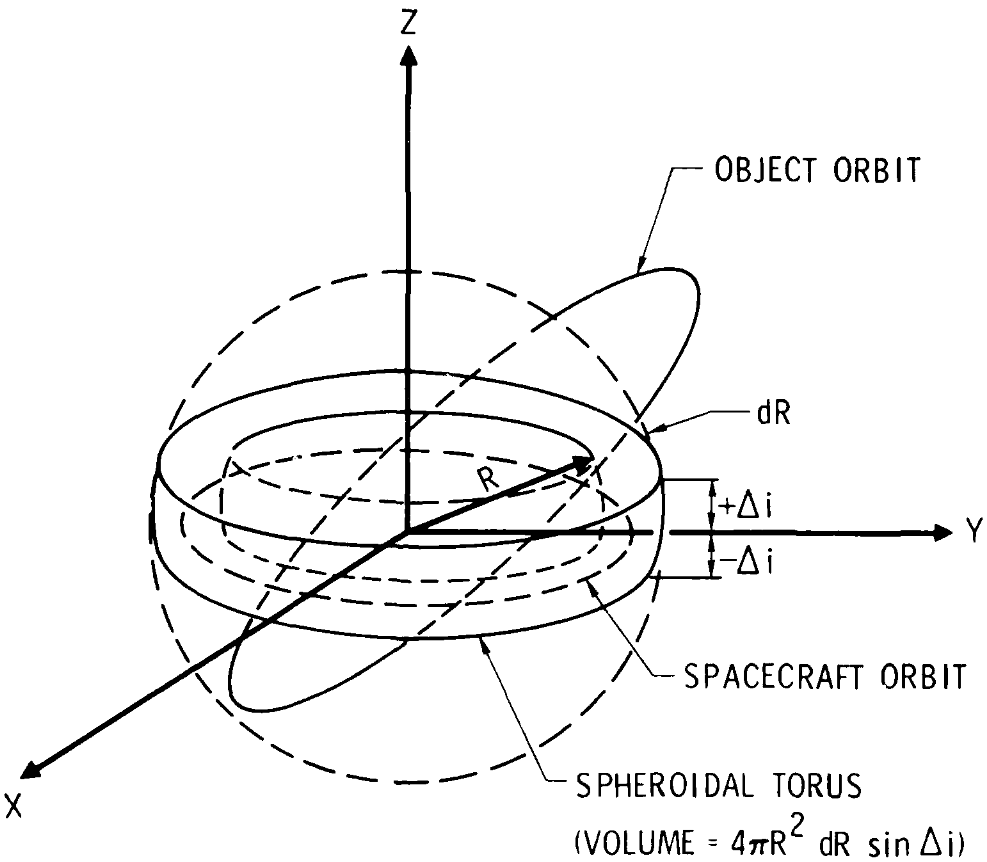

Fig. 16. Toroidal Geometry for Geosynchronous Orbits

where $A_1 = a_1/a_2$. Also, a_1, a_2, are the semimajor axes of the object and target orbits, and e_1 is the eccentricity of the object orbit.

The probability of the target spacecraft colliding with N objects in the torus (defined by an average inclination Δi_{av} of the objects' orbits relative to that of the target orbit) is equal to N times that given by Eq. (6). For example, if a set of 62 geosynchronous objects is considered with an average eccentricity $e_1 = 0.00113$ and orbit plane inclination $\Delta i = 1.07°$ relative to the equatorial plane, then the velocity relative to a spacecraft in a circular geosynchronous equatorial orbit at encounter is from Eq. (3) $v_r = 57.5$ m/sec where $a_1 = 1$ and r_x = geosynchronous radius. Consequently, a 1000 day probability of collision for a spacecraft of 50 m radius is by Eq. (6) equal to 3.88×10^{-5}.

Using Eq. (1), $v_r = 7$ km/sec, which is the average relative encounter velocity between satellites below 2000 km (Ref. 8) and the spatial density ρ in Fig. 7, the probability of collision for circular low altitude missions of 1000 days is given in Fig. 17 for the trackable population of 4174 objects and an estimated population of 8400 objects of smaller cross-section. The results show that the 1000 day probability of collision for a very large spacecraft (~50 m radius) is on the order of 4 to 8% and for a 20 m radius satellite it is on the order of 0.6 to 1.2%. However,for smaller spacecraft (~3 m radius), current probability of collision is an order of magnitude lower. The results for a sample of 62 to 620 objects in the geosynchronous corridor are given in Fig. 18 where an average relative velocity of only 36.5 m/sec was assumed. This velocity is the north-south (inclination) component of the average relative velocity. Average collision probabilities in the geosynchronous orbit are thus seen to be about three orders of magnitude lower than those at low altitudes. However, the effects of density variation with altitude, inclination (latitude) or longitude are not included in these results.

B. VARIABLE DENSITY METHOD

Figure 14 shows that the observed object density $\rho(h,\phi)$ is a function of height h above or below geosynchronous orbit and latitude ϕ. Since a satellite whose orbit plane is inclined to the equatorial plane spends only a

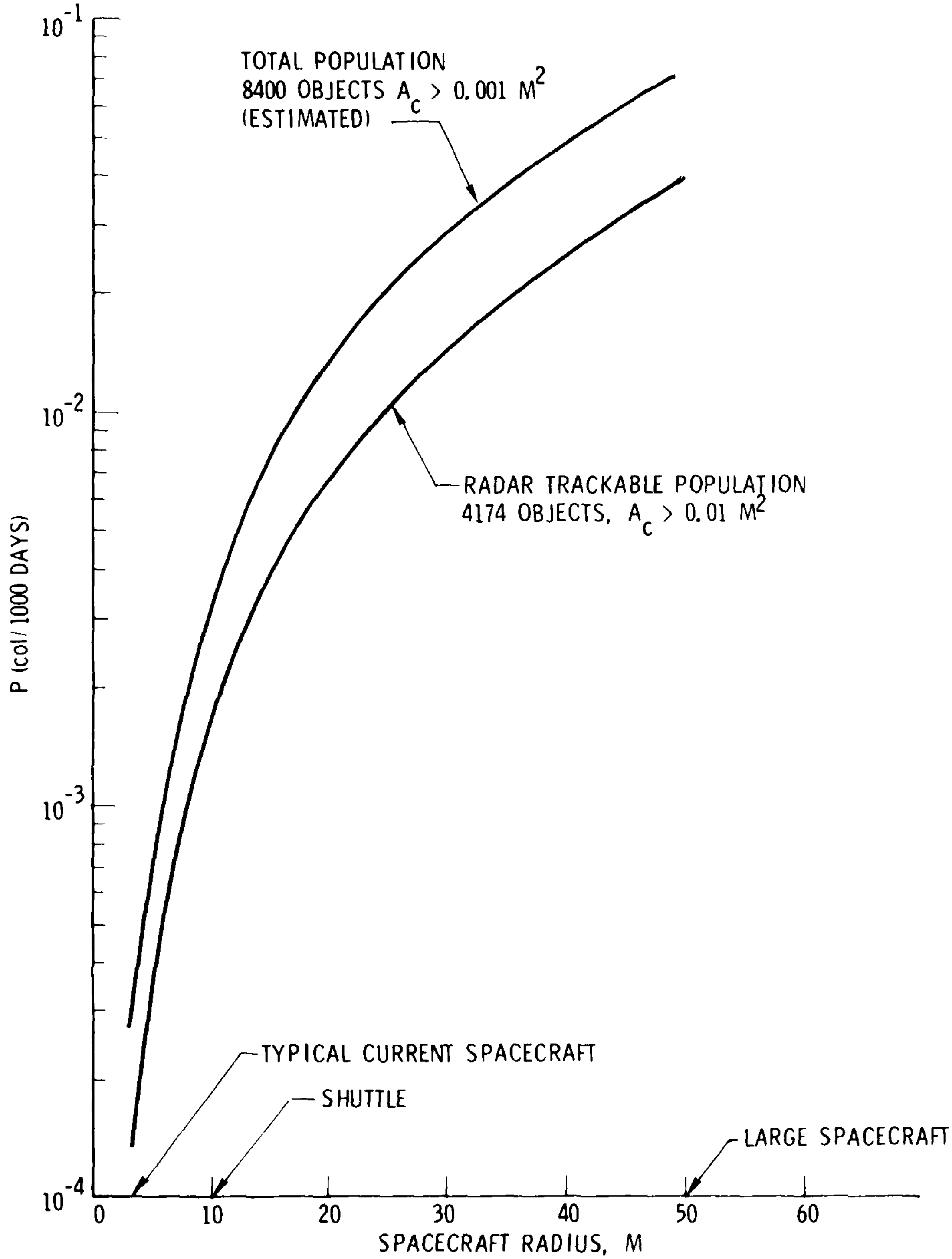

Fig. 17. Probability of Collision - Low Earth Orbits (800 to 1500 km) for 1000 Days

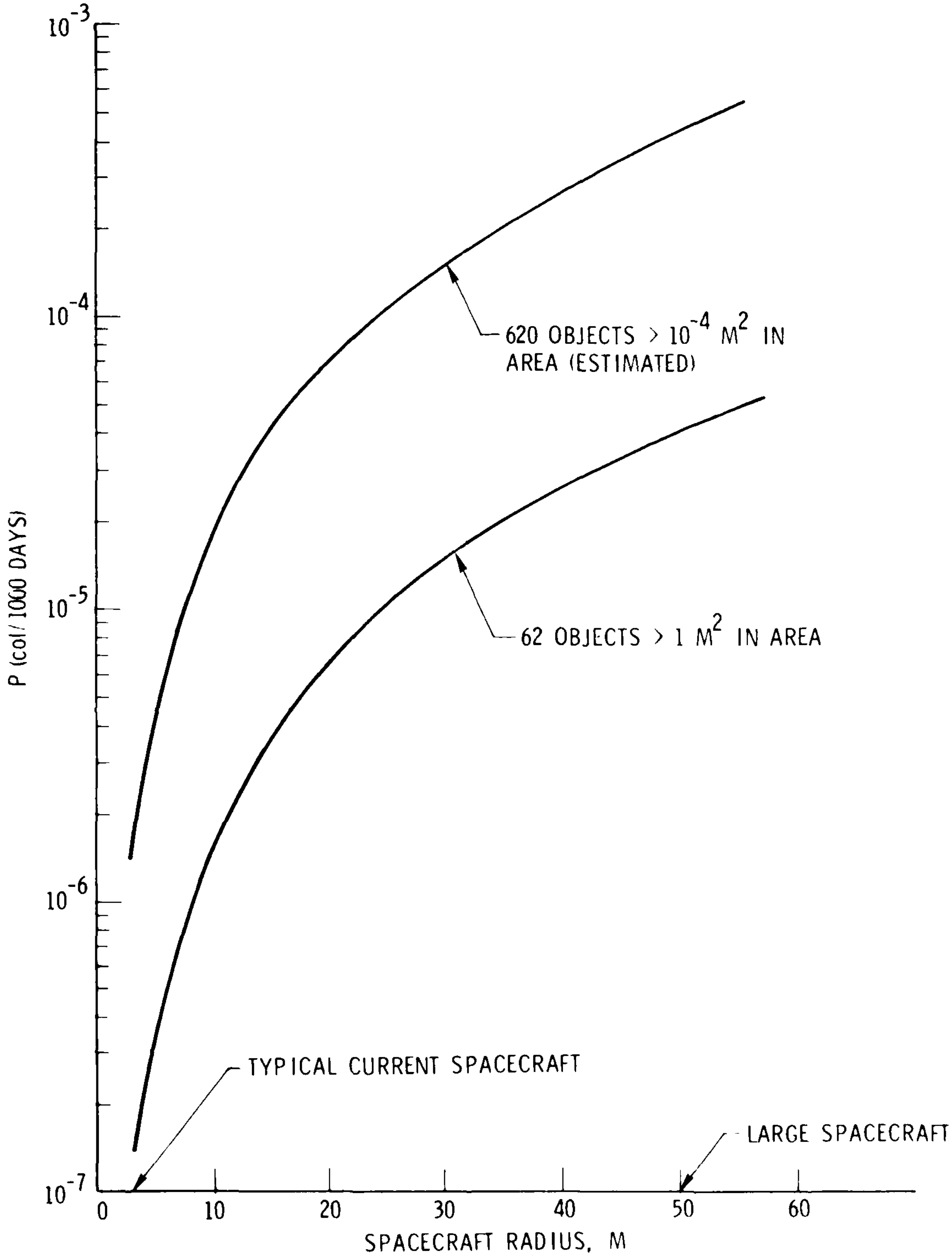

Fig. 18. Probability of Collision - Geosynchronous Orbits for 1000 Days

fraction of its period of revolution T near the equator where the density is greatest, the probability of collision is similarly affected. In general, the probability of collision in any altitude band $\Delta h = h_2 - h_1$, per one revolution of the satellite, is

$$p(col/rev) = A_c \bar{v}_r T \int_{h_1}^{h_2} \int_{-\phi}^{\phi} \rho(h,\phi) f(\phi) d\phi dh \tag{8}$$

where $\rho(h,\phi)$ is the object density function, $f(\phi)$ is a weighting function which can be derived from the time fraction spent by a satellite in a latitude band $\Delta\phi$ as shown in Fig. 19 and $\bar{v}_r$ is the average velocity of the target satellite relative to the objects of interest. For the case of a target satellite with inclination i and a set of geosynchronous objects with an average inclination $\bar{i}$ and average right ascension of the ascending node $\bar{\Omega}$, the angle Δi between the target orbit plane and that of the "average plane" of the objects is

$$\Delta i = \cos^{-1}(\cos i \cos\bar{i} + \sin i \sin\bar{i} \cos\Delta\Omega) \tag{9}$$

where

$\Delta\Omega = |\bar{\Omega} - \Omega|$

Ω = right ascension of the ascending node of the target satellite.

Since Δi will in general vary in time because of external perturbations, the average value of Δi is

$$\Delta i_{av} = \frac{\Delta i_{max} + \Delta i_{min}}{2} \tag{10}$$

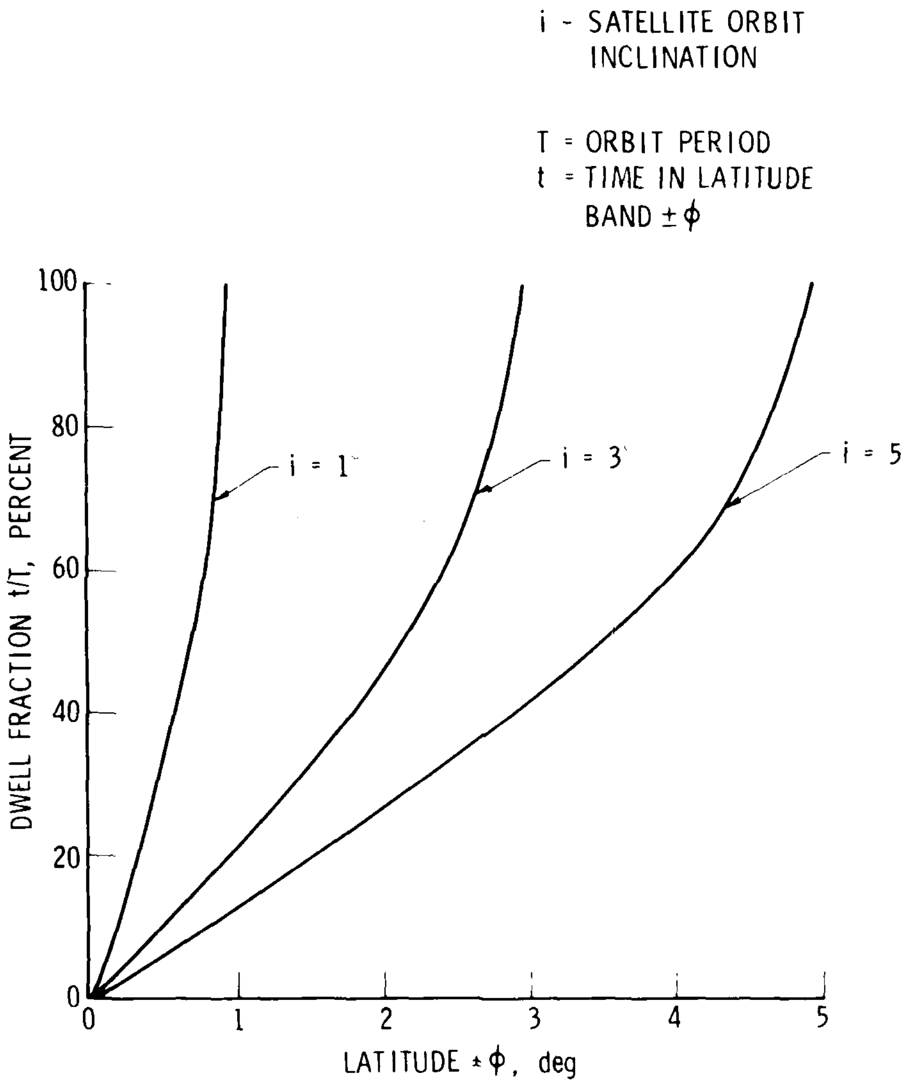

Fig. 19. Dwell Fraction vs. Latitude for Circular Orbits

where

$$\Delta i_{max} = i + \bar{i} \quad \text{when} \quad \Delta\Omega = \pi \tag{11}$$

and

$$\Delta i_{min} = |i - \bar{i}| \quad \text{when} \quad \Delta\Omega = 0 \tag{12}$$

Therefore,

$$\Delta i_{av} = \begin{cases} i & \text{for} \quad i > \bar{i} \\ \bar{i} & \text{for} \quad i < \bar{i} \end{cases} \tag{13}$$

The average relative velocity v_r for the case of nearly circular geosynchronous orbits can be approximated by Eq. (5) because the normal (out-of plane) or north-south component predominates.

Equation (8) has been evaluated approximately for circular orbits with $i = 1°$, $3°$ and $5°$ and object densities of Fig. 14 for different altitude bands above and below geosynchronous orbit. The results, given in Fig. 20, are valid for a typical small satellite (effective collision radius R_S = 20 ft (6.1 m)) and a mission duration of 1000 days. The results for other values of R_S are proportional to the square of the effective radius of collision and time. The collision probability for a target satellite in an elliptic geosynchronous orbit can be obtained by averaging the results of Fig. 18 as shown in Fig. 21.

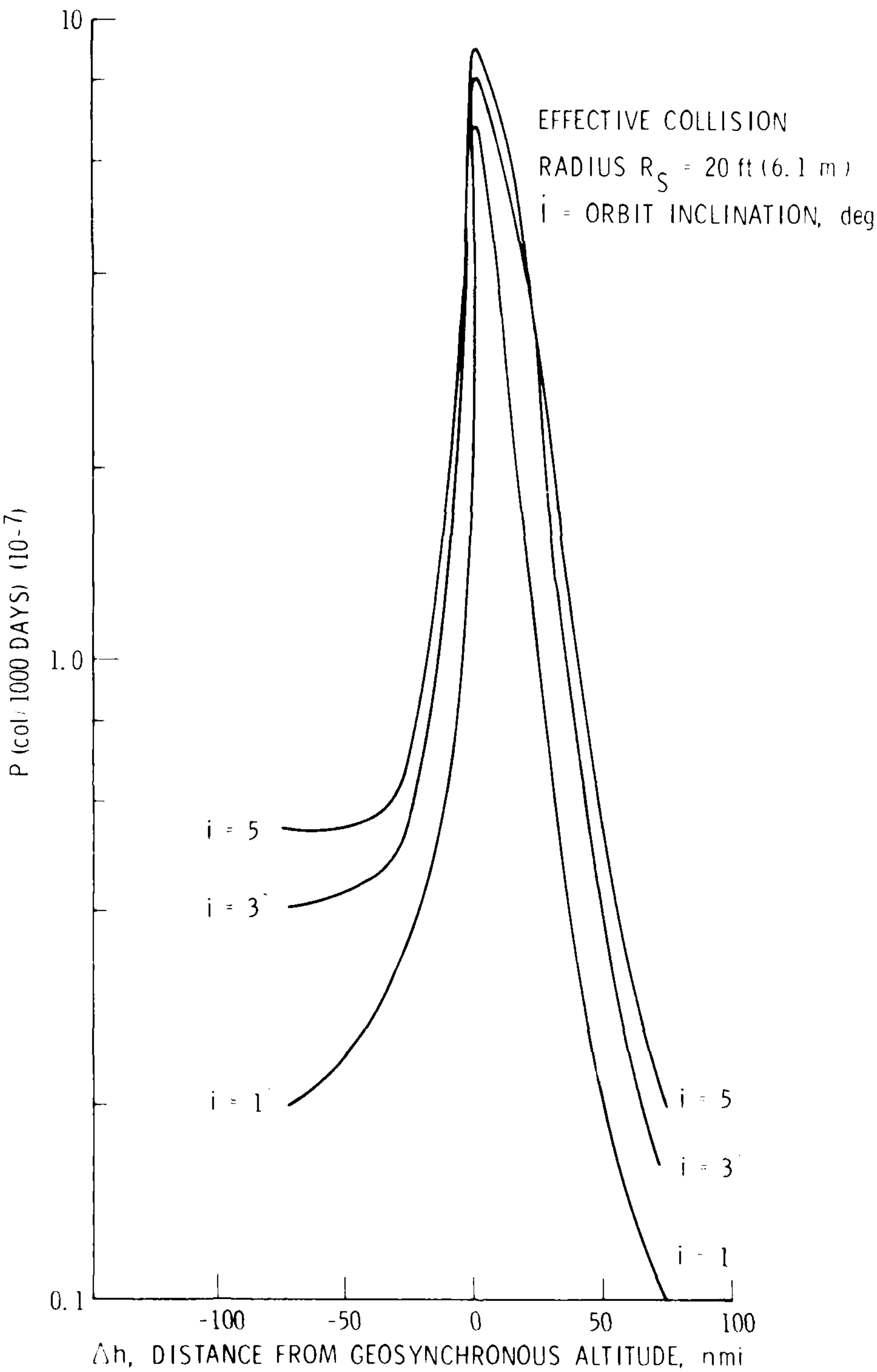

Fig. 20. Collision Probability for Objects in Circular Geosynchronous Orbits in 1000 Days

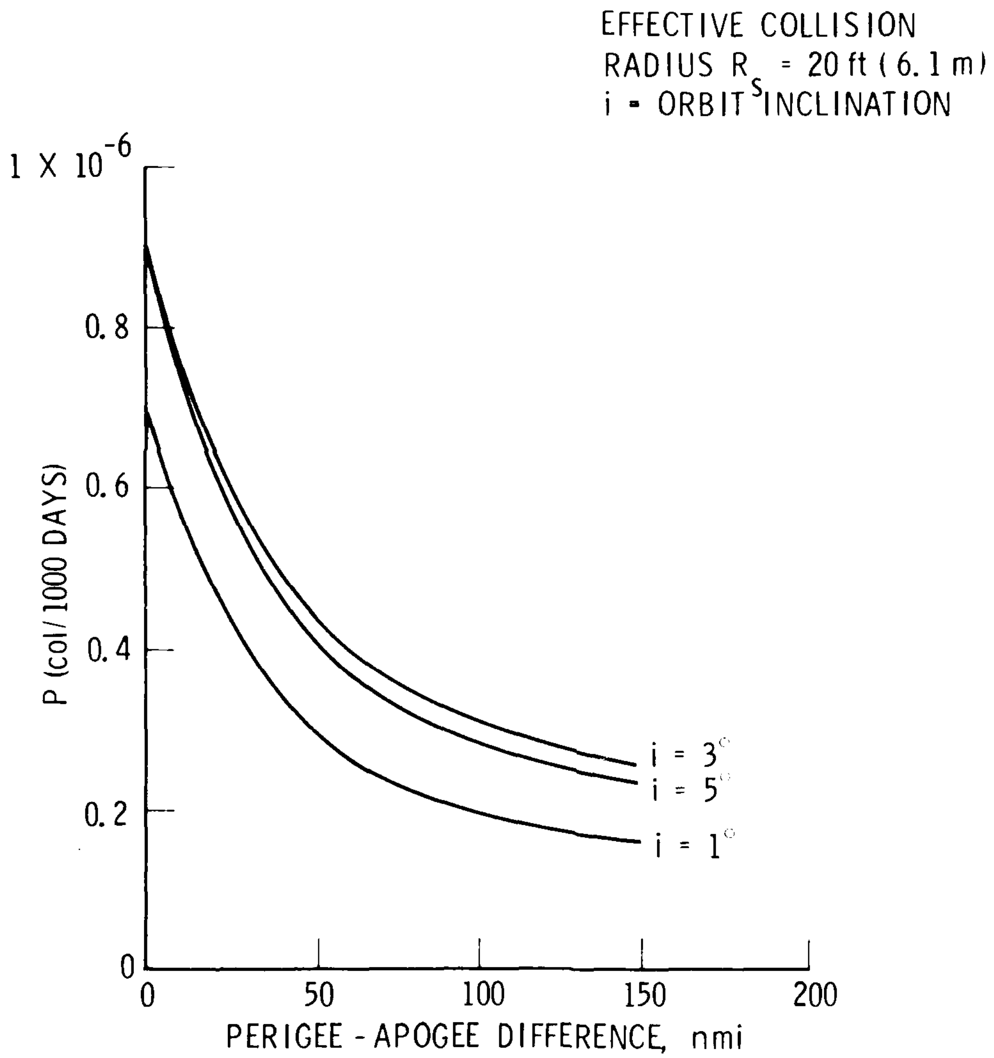

Fig. 21. Collision Probability for Objects in Eccentric Geosynchronous Orbits in 1000 Days

C. DISTANCE OF CLOSEST APPROACH METHOD

1. GENERAL CONSIDERATIONS

A collision between two objects can take place at or near a trace intersection point if the distance of closest approach R_{MIN} is equal to or is less than the effective collision radius R_S. For satellites in circular orbits with a mutual orbit plane inclination α, R_{MIN} occurs twice per revolution in the vicinity of the intersection between the orbit planes (nodal axis) as illustrated in Fig. 22. For each instant when satellite 1 is at or near the nodal axis, satellite 2 is at a position 4, 3, 2 or 1 corresponding to an R_{MIN} for that pass. The angular increment $\Delta u = n_1|(T_2 - T_1)|$ where n_1 is the mean motion of satellite 1 and T_1, T_2 are the periods of revolution for satellites 1 and 2, respectively. The angular change Δu per revolution is typically a fraction of a degree for geosynchronous satellites. For example, R_{MIN} for north and south bound passes of OPS 6391 (SDC object No. 10669) and WESTAR-A (SCD object No. 7250), is given in Table 2 for several days in April of 1980 as was determined approximately via the numerical simulation described in Ref. 14. Different R_{MIN} values can thus be seen to have occurred before and after the lowest value R_{MIN} = 5.28 nmi of 21 April 1980. The probability of collision between the objects for each pass is, in general, a function of R_{MIN}, the tracking uncertainty σ in the location of each object and the effective collision radius R_S. The latter can be defined as one half the sum of the maximum dimensions for both objects. For $\sigma = 0$ and $R_{MIN} > R_S$ no collision can take place. For $\sigma \neq 0$, there is a nonzero probability of collision.

2. MISS DISTANCE AND POSITION UNCERTAINTY

An approximate collision probability method, described briefly in (Ref. 15), considers the effects of the uncertainties associated with the three dimensions (coordinates) of the miss distance R_{MIN}. It is assumed that the uncertainties are Gaussian (normal) with zero biases and equal variance and that they are uncorrelated. The assumption is applied to the position data of each of the tracked satellites. In view of this and the fact that the orientation of the coordinate system containing the distance of closest

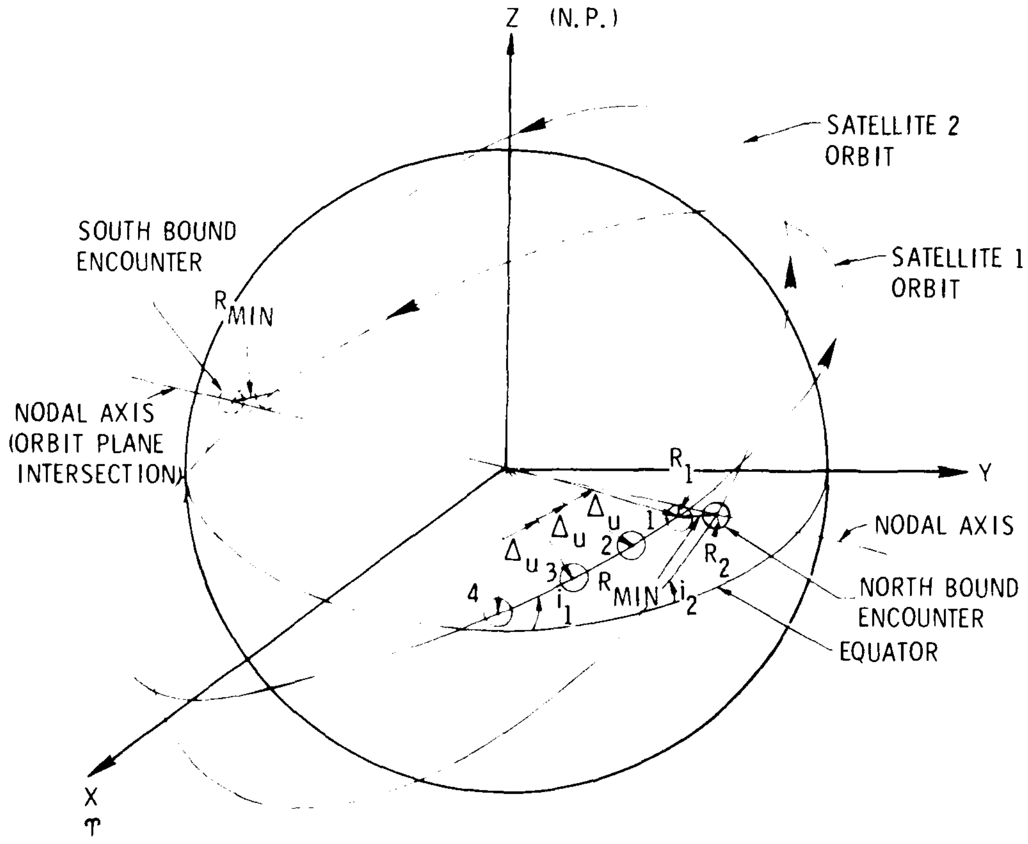

Fig. 22. Encounter Geometry for Mutually Inclined Circular Orbits

Table 2. Close Encounters Between OPS 6391 and WESTAR-A Geosynchronous Satellites

R_{MIN} – (Relative Minimum) (nmi/km)	Date	10669 (OPS 6391) lat (deg)	10669 (OPS 6391) long. (deg)	10669 (OPS 6391) alt (nmi)	7250 (Westar-A) lat (deg)	7250 (Westar-A) long. (deg)	7250 (Westar-A) alt (nmi)
26.55/ 49.17	12. Apr 9:42:58.1	.0317	-99.2406	19329.05	.0337	-99.1751	19323.83
14.31/ 26.50	12. Apr 21:41: 8.0	-.0341	-99.1765	19316.98	-.0336	-99.1437	19322.82
23.63/ 43.77	13. Apr 9:38:58.3	.0316	-99.2429	19329.07	.0334	-99.1850	19323.84
11.68/ 21.63	13. Apr 21:37: 5.7	-.0332	-99.1791	19316.98	-.0328	-99.1537	19322.83
20.76/ 38.45	14. Apr 9:35: .5	.0307	-99.2455	19329.09	.0322	-99.1950	19323.86
9.26/ 17.16	14. Apr 21:33: 5.2	-.0315	-99.1817	19316.98	-.0312	-99.1636	19322.84
17.94/ 33.22	15. Apr 9:31: 4.1	.0290	-99.2479	19329.10	.0303	-99.2047	19323.87
7.25/ 13.43	15. Apr 21:29: 5.7	-.0295	-99.1839	19316.98	-.0292	-99.1732	19322.84
15.16/ 28.08	16. Apr 9:27: 8.2	.0272	-99.2499	19329.12	.0282	-99.2141	19323.88
6.02/ 11.15	16. Apr 21:25: 6.3	-.0274	-99.1858	19316.99	-.0272	-99.1824	19322.85
12.44/ 23.05	17. Apr 9:23:12.2	.0256	-99.2515	19329.13	.0264	-99.2231	19323.90
6.08/ 11.25	17. Apr 21:21: 6.6	-.0258	-99.1873	19316.99	-.0257	-99.1913	19322.86
9.84/ 18.22	18. Apr 9:19:15.8	.0247	-99.2529	19329.14	.0253	-99.2319	19323.91
7.41/ 13.73	18. Apr 21:17: 6.6	-.0249	-99.1888	19317.00	-.0250	-99.2002	19322.87
7.48/ 13.86	19. Apr 9:15:19.1	.0246	-99.2544	19329.16	.0250	-99.2410	19323.92
9.53/ 17.65	19. Apr 21:13: 6.2	-.0251	-99.1907	19317.01	-.0252	-99.2096	19322.88
5.73/ 10.62	20. Apr 9:11:22.2	.0255	-99.2566	19329.17	.0256	-99.2508	19323.93
12.04/ 22.29	20. Apr 21: 9: 5.6	.0260	-99.1934	19317.02	-.0262	-99.2198	19322.89
5.28/ 9.78	21. Apr 9: 7:24.9	.0270	-99.2598	19329.18	.0269	-99.2615	19323.94
14.74/ 27.31	21. Apr 21: 5: 4.5	-.0274	-99.1971	19317.03	-.0277	-99.2312	19322.90
6.43/ 11.90	22. Apr 9: 3:27.2	.0288	-99.2642	19329.19	.0285	-99.2735	19323.96
17.56/ 32.52	22. Apr 21: 1: 2.9	-.0290	-99.2021	19317.03	-.0294	-99.2438	19322.90

approach at encounter is arbitrary, a plane xy which is normal to the relative velocity vector and which contains the vector of closest approach R_{MIN} can always be found. The bi-variate normal density function for this case can be expressed as (Ref. 16)

$$f(x,y) = \left(\frac{e^{-\frac{x^2}{2\sigma^2}}}{\sigma\sqrt{2\pi}}\right)\left(\frac{e^{-\frac{y^2}{2\sigma^2}}}{\sigma\sqrt{2\pi}}\right)$$

$$= \frac{1}{2\pi\sigma^2}\, e^{-\frac{1}{2}\left(\frac{R_{MIN}}{\sigma}\right)^2} \tag{14}$$

where

$$R_{MIN} = \left(X^2_{min} + Y^2_{min}\right)^{1/2}$$

Since a collision can occur only if

$$\left.\begin{aligned} Y_{min} - R_s \leq y \leq R_s + Y_{min} \\ X_{min} - R_s \leq x \leq R_s + X_{min} \end{aligned}\right\} \tag{15}$$

where X_{min}, Y_{min} are the coordinates of R_{MIN} and where R_s is the effective collision radius for both satellites, the probability of collision is

$$p(\text{col}) = \int_{(X_{min} - R_s)}^{(X_{min} + R_s)} \int_{(Y_{min} - R_s)}^{(Y_{min} + R_s)} f(x,y)\,dy\,dx \tag{16}$$

$$\approx \frac{2}{\pi}\left(\frac{R_s}{\sigma}\right)^2 e^{-\frac{1}{2}\left(\frac{R_{MIN}}{\sigma}\right)^2} \tag{17}$$

for $R_s \ll R_{MIN}$.

Equation (17) represents the probability of collision between two satellites per encounter when the distance of closest approach R_{MIN}, the 1 σ tracking uncertainty in the position of each satellite, and the effective radius of collision R_s are given.

A similar result can be obtained by orienting the x, y coordinates along $\vec{R}_{MIN}$ and normal to it respectively. The probability of collision is then

$$p(\text{col}) = p_x p_y \tag{18}$$

where

$$p_x = p[A \leq x \leq B]$$

$$= p\left[\frac{A}{\sigma} \leq x' \leq \frac{B}{\sigma}\right]$$

$$= \frac{1}{\sqrt{2\pi}\sigma} \int_{A/\sigma}^{B/\sigma} e^{-\frac{\mu^2}{2}}\,du$$

= probability of collision along x

$$p_y = p[-R_s \leq y \leq R_s]$$

$$= p[-\frac{R_s}{\sigma} \leq y' \leq \frac{R_s}{\sigma}]$$

$$= \frac{1}{\sqrt{2\pi}\sigma} \int_{-R_s/\sigma}^{R_s/\sigma} e^{-\frac{u^2}{2}} du$$

= probability of collision in a direction normal to $\vec{R}_{MIN}$

Here

$$A = R_{MIN} - R_s$$

$$B = R_{MIN} + R_s$$

and A/σ, B/σ and R_s/σ are standardized Gaussian variables.

Assuming now that the probability of collision at j-th closest approach is $p_j(col)$ the probability of miss is

$$p_j(miss) = 1 - p_j(col) \tag{19}$$

The probability of missing at all n closest approaches is

$$p(miss/n) = \prod_{j=1}^{n} [1 - p_j(col)] \tag{20}$$

if all probabilities are independent. Therefore, the probability that there will be at least one collision during this period of encounter is

$$p(col) = 1 - p(miss/n)$$

$$\approx \sum_{j=1}^{n} p_j(col) \tag{21}$$

when all $p_j(col) \ll 1$.

A plot of Eq. (17) for R_s = 20, 50 and 100 ft is given in Figs. 22 to 26 as a function of σ with R_{MIN} as a parameter. It can be seen that a maximum probability of collision occurs when

$$\sigma = \frac{R_{MIN}}{\sqrt{2}} \tag{22}$$

which is plotted as a function of R_s/R_{MIN} in Fig. 28. The use of Eqs. (17) and (21) is illustrated in Fig. 29 for the case of the close encounters between the WESTAR-A and the OPS 6391 satellites given in Table 2. The collision probabilities for several passes are plotted as a function of σ. The maximum probability of collision for 17 passes is given as the sum of the maximum probabilities for each pass. Assuming no correlation between passes, the maximum (upper-bound) probability of collision for these encounters is 2.0×10^{-6} for the 8-day time period.

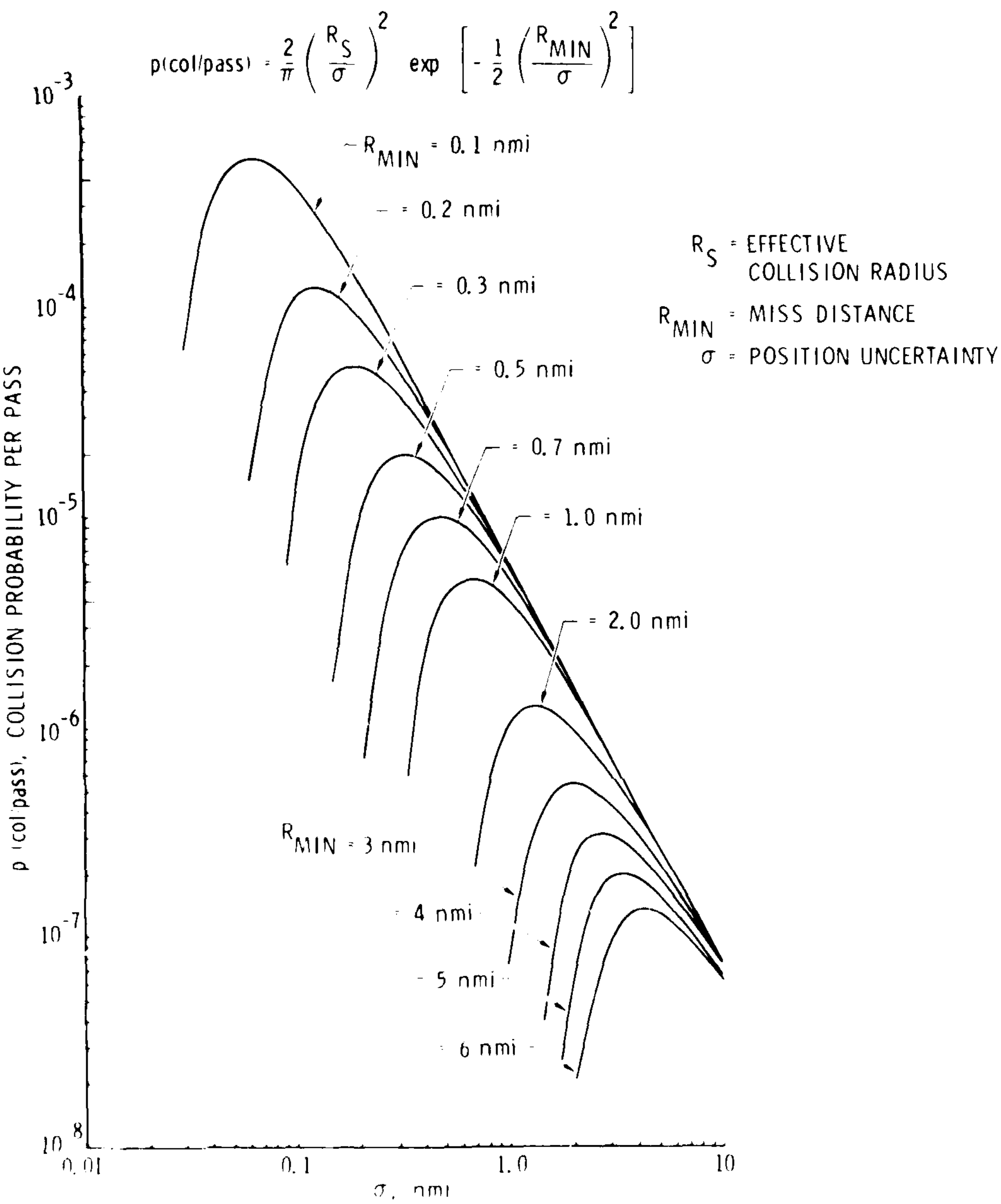

Fig. 23. Collision Probability as a Function of Position Uncertainty and Miss Distance (R_S = 20 ft)

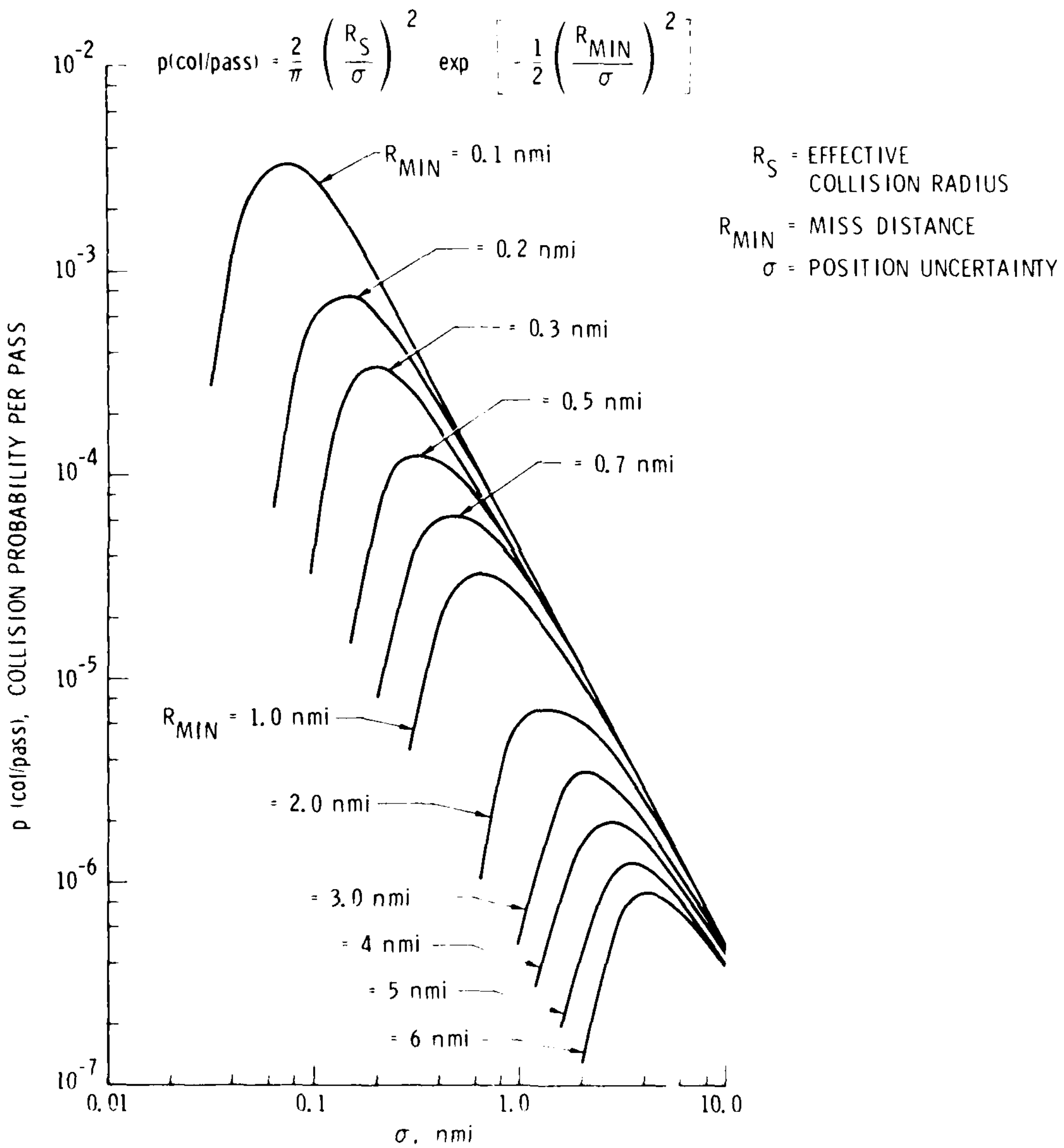

Fig. 24. Collision Probability as a Function of Position Uncertainty and Miss Distance (R_S = 50 ft)

$$p(col/pass) = \frac{2}{\pi}\left(\frac{R_S}{\sigma}\right)^2 \exp\left[-\frac{1}{2}\left(\frac{R_{MIN}}{\sigma}\right)^2\right]$$

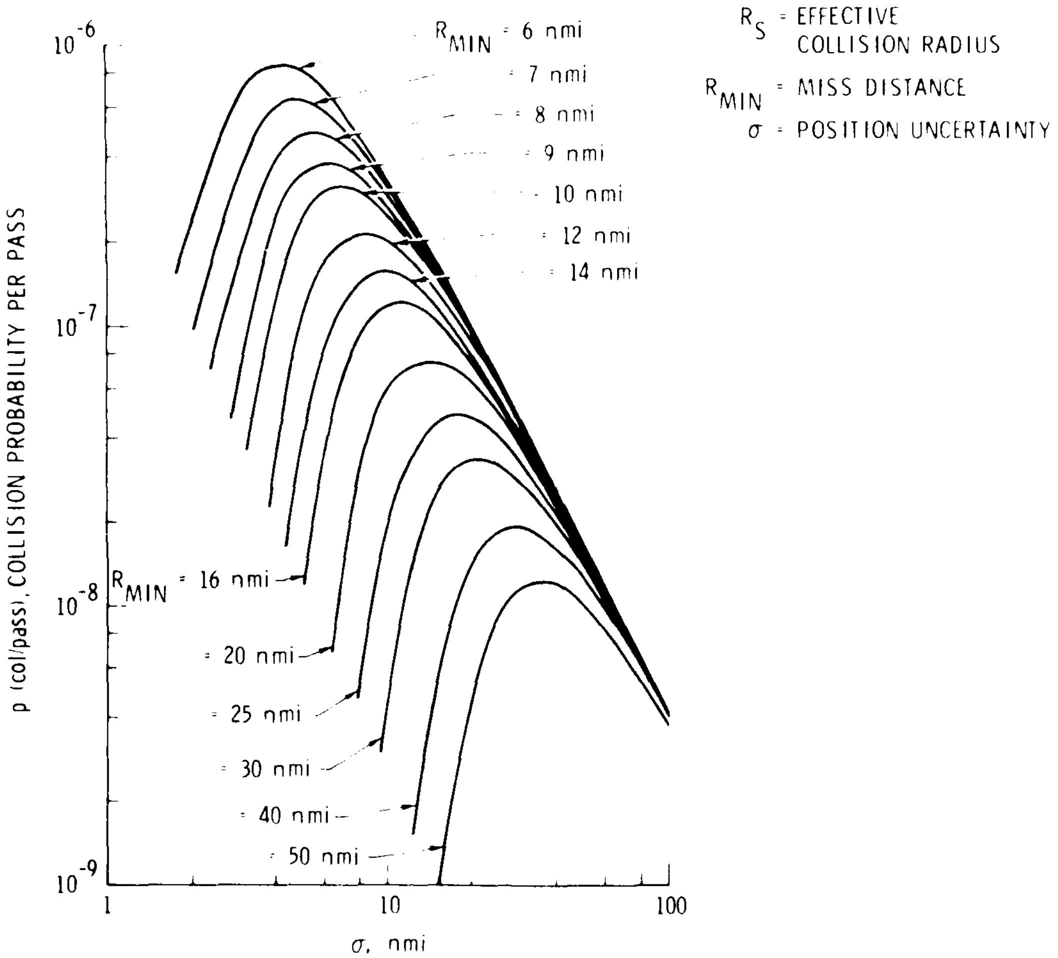

Fig. 25. Collision Probability as a Function of Position Uncertainty and Miss Distance (R_S = 50 ft), Continued

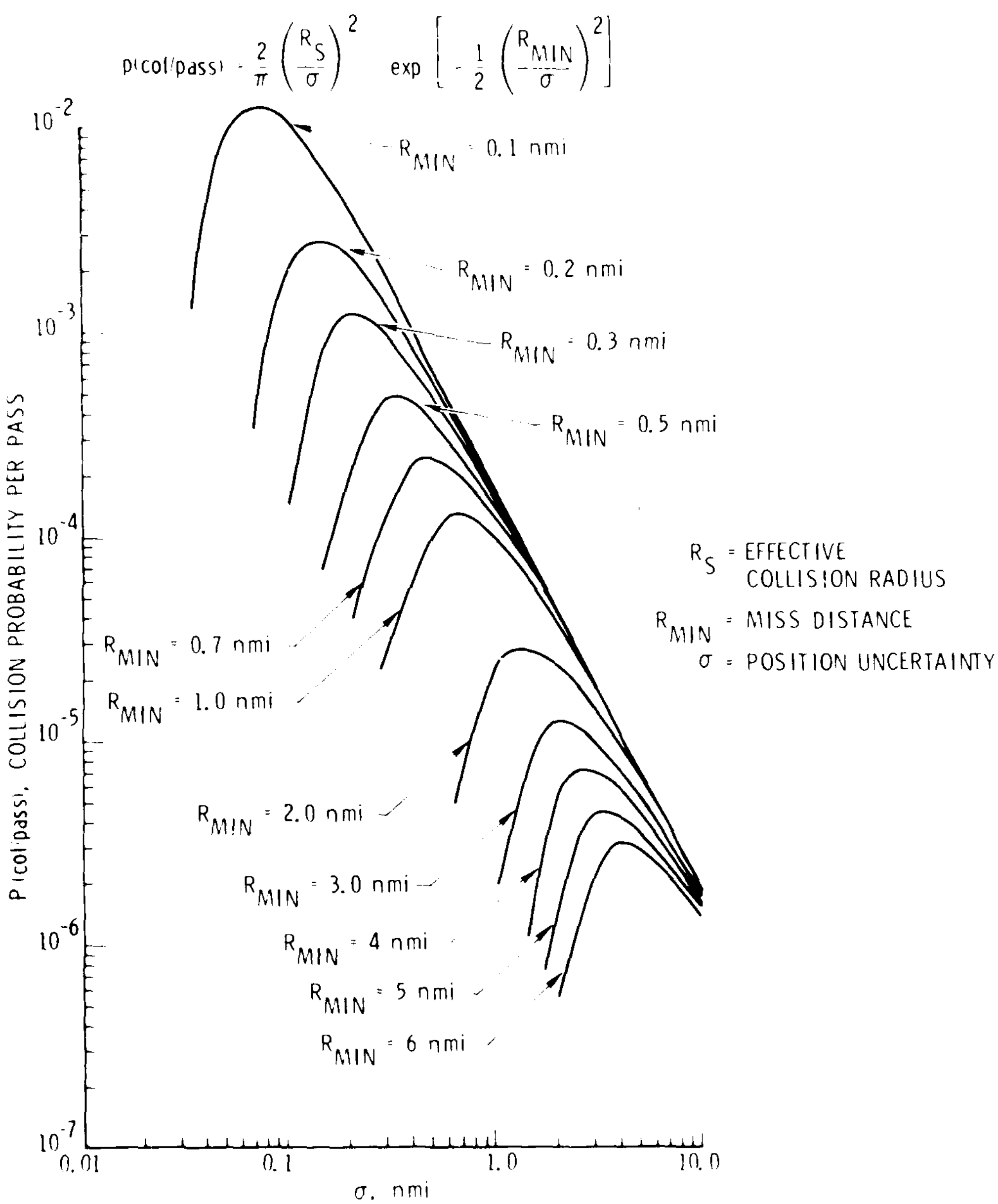

Fig. 26. Collision Probability as a Function of Position Uncertainty and Miss Distance (R_S = 100 ft)

$$p(\text{col/pass}) = \frac{2}{\pi}\left(\frac{R_S}{\sigma}\right)^2 \exp\left[-\frac{1}{2}\left(\frac{R_{MIN}}{\sigma}\right)^2\right]$$

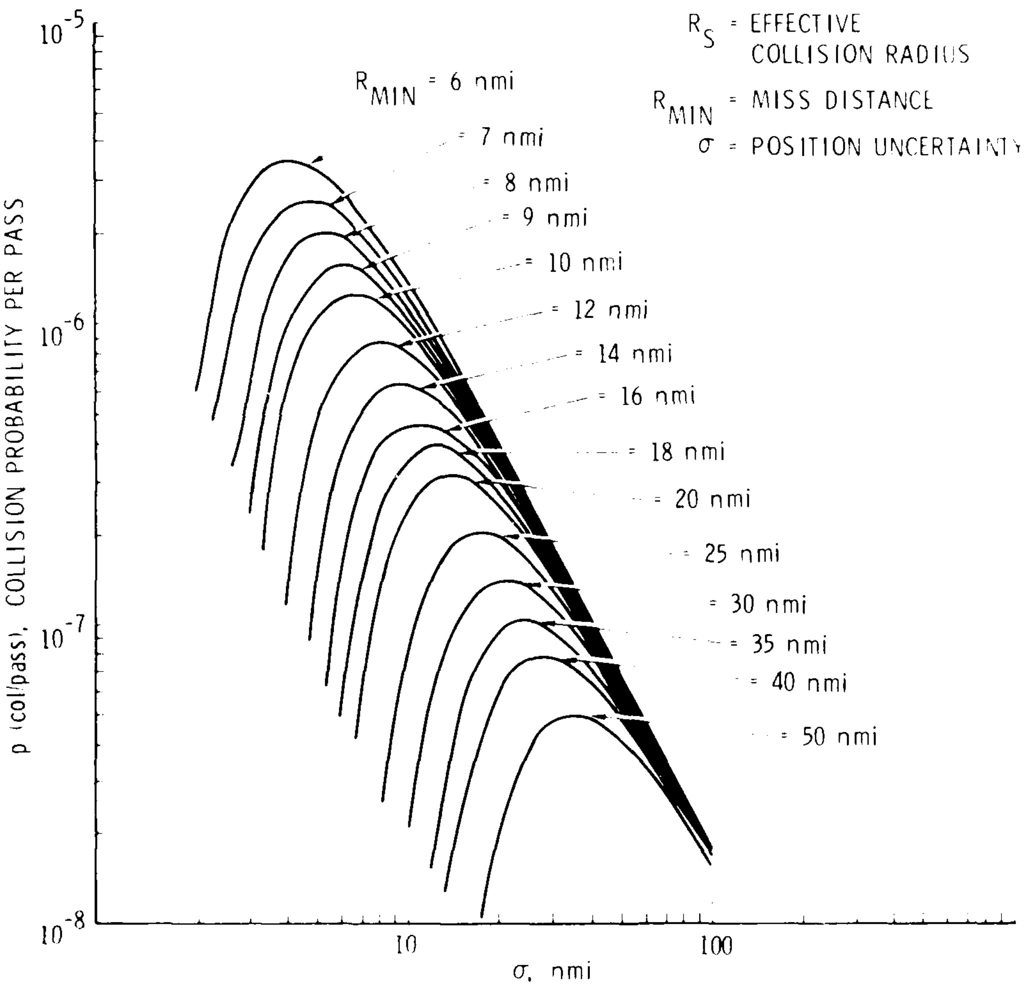

Fig. 27. Collision Probability as a Function of Position Uncertainty and Miss Distance (R_S = 100 ft), Continued

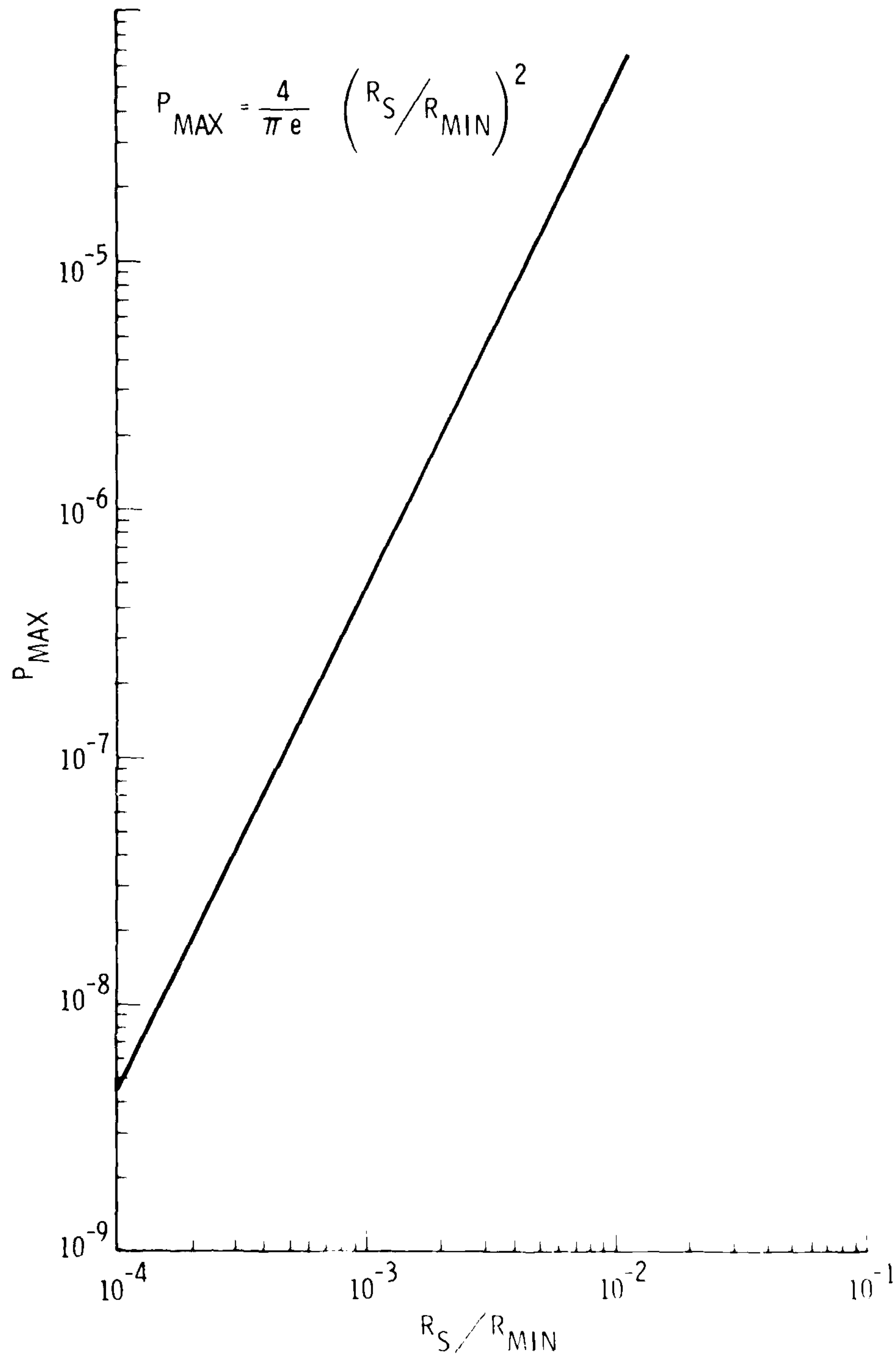

Fig. 28. Maximum Collision Probability Per Pass (P_{max}) as Function of Effective Collision Radius to [illegible] Distance Ratio (R_S/R_{min})

[EFFECTIVE COLLISION RADIUS $R_S = 30$ ft, $p(col)_{max} = \sum_{i=1}^{17} P_{imax} = 2.0 \times 10^{-6}$]

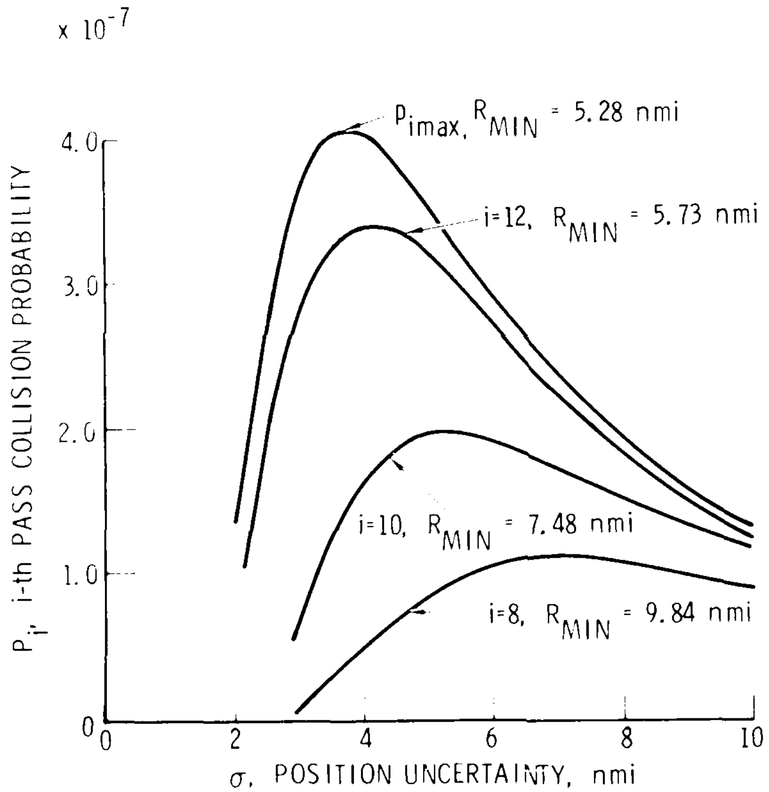

Fig. 29. WESTAR-A/OPS 6391 Collision Probability During the April 14 to April 23, 1980 Encounters in Geosynchronous Orbit

IV. SUMMARY AND CONCLUSIONS

A summary of the present and projected probabilities of collision for a ten meter radius spacecraft in low earth orbit (LEO) and the geosynchronous corridor (GEO) is given in Table 3. It can be seen that the probability of collision in low earth orbits is currently on the order of 0.15 to 0.3% for a 1000-day mission. Another way of interpreting the probability of 0.3% is that one of 90 such spacecraft would be expected to experience a collision in 10 years. Probabilities for the 1985 to 1995 time frame are on the order of 2.5 to 7.3 times current values on the basis of an assumed debris growth rate of 13% per year. On the other hand, the results for the geosynchronous orbit are some three orders of magnitude lower in value mainly because of lower relative velocities at encounter. These results, however, do not include the effects of ascending node concentrations at certain longitudes. The calculated probabilities of collision at low altitude are also likely to be too low due to the noninclusion of many smaller particles believed to be a result of satellite explosions and ASAT tests.

The picture emerging from this study indicates that the cluttering of space with debris must be reduced in the future to minimize the collision hazard and improve spacecraft survivability. It appears that the current debris growth rates of 9 to 13% are excessive and that the associated collision hazards, particularly for larger spacecraft, will become unacceptable if these growth rates remain unchanged. There is little doubt that larger satellites and space stations will be built in the future, because of increasing demands for more and better space communications, meteorology, navigation, and remote sensing.

The question of "what solutions can be postulated" can be answered only by resolution of the space debris issues falling into three categories: 1) satellite and vehicle design, 2) operational procedures and practices, and 3) national and international policies and treaties. In the area of vehicle design the principal approaches should consider space systems for litter-free

Table 3. Summary of Present and Projected Collision Probabilities for a 1000-Day Mission

Probability of Collision with Trackable Objects	1980 (4174 objects)	1985 (~10000 objects) (multiplying factor)	1995 (30000 objects) (multiplying factor)
Ten meter radius spacecraft in GEO(a)	10^{-6} to 10^{-5}	2.5	7.3
Fifty meter radius spacecraft in GEO	4×10^{-5} to 4×10^{-4}	2.5	7.3
Ten meter radius spacecraft in LEO(b)	1.5×10^{-3} to 3×10^{-3}	2.5	7.3
Fifty meter radius spacecraft in LEO	4×10^{-2} to 8×10^{-2}	2.5	7.3

(a) GEO - Geosynchronous Orbit

(b) LEO - Low Earth Orbit

separation, reusability, retrievability, earth escape or destructive reentry into the atmosphere. The feasibility of debris collection systems should be examined.

In the operational approach and procedure areas, consideration should be given to satellite separation techniques (use of nonintersecting orbits, etc.), avoidance of crowded regions of space, and the disposal of spent satellites to "graveyard" orbits. Accidental or deliberate destruction of spacecraft should be minimized. Some of the possible approaches are summarized in Fig. 30. In short, Planet Earth appears to need a consistent and universally observed space object management policy which could ensure that future missions would be protected from unacceptable collision hazards in orbit.

SATELLITE POSITION MANAGEMENT POLICY

1. ESTABLISH CLOSE APPROACH MONITORING CAPABILITY
2. ALERT SATELLITE USERS/OPERATORS AND OTHER APPROPRIATE AGENCIES WHENEVER PLANS ARE MADE TO REPOSITION A SATELLITE
3. REDUCE NUMBER OF DEBRIS OBJECTS DURING LAUNCHING, ORBIT INJECTION AND OPERATION OF SATELLITES (e.g. SHROUDS, COVERS, PARTS JETTISONING, ETC.)
4. REMOVE INACTIVE SATELLITES FROM ORBIT OR PLACE IN DISPOSAL ORBITS
5. TARGET BOOSTER STAGES ABOVE OR BELOW MISSION ORBIT
6. MINIMIZE POSSIBILITY OF ROCKET STAGE OR PAYLOAD BREAKUP OR EXPLOSION
7. DETERMINE EFFECTS OF ACTUAL OR PLANNED EXPLOSIONS ON THE PROBABILITY OF INADVERTENT COLLISIONS
8. USE NONINTERSECTING ORBITS
9. PERFORM COLLISION AVOIDANCE MANEUVERS WHEN NECESSARY

Fig. 30. Operational Procedures to Minimize Collision Hazard in Space

APPENDIX

SYNCHRONOUS SATELLITE CATALOG

(28 April 1980)

ALPHABETICAL

(Ref. 3)

SYNCHRO[illegible] SATELLITES FOR SAT[illegible]112, [illegible] APR 8[illegible]					EPOCH (1)	D (2)	LATITUDE (3)	LONGITUDE (3)	HEIGHT (3)	APOGEE (4)	PERIGEE (4)	INCL (4)	DRIFT (5)
05479	72 90	A	ANIK 1 (TELESAT)	CANADA	80118.6624	2.3	-0.0516	-103.9965	19324	19329	19324	0.04	-0.0073
06437	73 23	A	ANIK 2 (TELESAT B)	CANADA	80109.7208	2.3	-0.0096	-106.4438	19323	19329	19320	0.07	-0.0062
07732	75 38	A	ANIK 3 (TELESAT C)	CANADA	80113.7308	5.3	-0.0089	-114.0171	19324	19327	19322	0.02	-0.0078
11153	78116	A	ANIK 4	CANADA	80116.7088	2.3	0.0124	-109.0013	19323	19330	19320	0.07	-0.0073
02608	66110	A	ATS 1	NASA	80117.9279	1.1	4.4263	-149.3470	19326	19326	19321	9.78	0.0175
03029	67111	A	ATS 3	NASA	80119.8225	3.0	7.5032	-105.6805	19299	19353	19287	8.36	-0.0071
04068	69 69	A	ATS 5	NASA	80118.7582	3.2	5.9994	-69.2990	19354	19352	19285	6.02	0.0216
07318	74 39		ATS-F	NASA	80112.4966	5.5	-2.0950	89.3404	19001	19149	18993	2.84	6.1489
07324	74 39	A	ATS-F R/B (2)	NORAD	80 98.8729	23.1	2.9214	-38.7622	18954	20237	18220	2.90	1.5699
10792	78 32	A	BSE	JAPAN	80 71.2390	47.8	-0.0298	101.7170	19386	19831	18799	0.19	-0.0198
09047	76 73	A	COMSTAR 1 D2	NASA	80116.4701	2.3	0.0465	-95.0762	19325	19329	19323	0.08	-0.0142
08838	76 42	A	COMSTAR 1-D1	NASA	80116.7611	2.2	0.0886	-127.8639	19322	19328	19322	0.07	0.0072
10975	78 71	A	COMSTAR 1D3	NASA	80116.6476	2.4	0.0429	-86.9549	19326	19328	19324	0.07	-0.0084
11676	79 97	R	COS 778 R/B	NORAD	80116.0443	3.0	-0.8569	-158.9336	19383	19433	19295	3.42	-0.9786
07229	74 17	A	COSMOS 637	USSR	80 95.1980	23.8	-0.3278	-157.8969	19192	19339	19139	4.44	1.8043
11557	74 17	R	COSMOS 637 R/B	NORAD	80114.1283	4.9	-2.0721	177.0229	19124	19309	19124	4.31	2.6008
08357	75 97	A	COSMOS 775	USSR	80116.3013	2.7	-3.3495	108.9472	19466	19479	19179	3.90	-0.1037
10516	77116	A	CS	JAPAN	79344.4147	132.6	0.0303	101.8031	19355	19333	19305	0.08	-0.0996
08888	76 4	A	CTS-A	CANADA	80112.0346	7.0	0.2076	-125.0066	19341	19345	19288	1.80	0.1885
11251	79 9	A	ECS	JAPAN	80 16.0146	103.0	-0.4707	25.7803	18126	20931	15857	1.07	22.0816
11735	80 18	A	ECS 2	JAPAN	80 54.3111	64.7	-0.3010	5.0701	19335	19659	19110	0.50	-1.3818
09973	76107	A	EKRAN	USSR	80 95.4942	23.5	-1.1532	71.9928	19445	19449	19187	2.27	0.1763
11559	76107	R	EKRAN 1 R/B	NORAD	80118.1595	3.8	-1.6925	174.2120	19160	19179	19122	2.23	4.9697
10365	77 92	A	EKRAN 2	USSR	80116.4049	2.6	-0.9187	85.7330	19206	19444	19190	1.55	0.1809
11571	77 92	R	EKRAN 2 R/B	NORAD	80117.7716	1.2	1.4743	-43.1920	19141	19212	19134	1.58	3.6367
11273	79 15	A	EKRAN 3	USSR	80116.1386	2.9	-0.3625	97.9966	19367	19439	19242	0.51	0.0472
11591	79 87	A	EKRAN 4	USSR	80116.1310	2.9	0.0518	99.9220	19277	19374	19276	0.04	-0.0195
[illegible]	64		[illegible]	[illegible]	80113.[illegible]	[illegible]	-67.9457	28.5767	32427	35678	1857	65.08	13.9425

PRECEDING PAGE BLANK-NOT FILMED

[illegible]	[illegible]		[illegible]	[illegible]	[illegible]	[illegible]	LATITUDE	LONGITUDE	HEIGHT	APOGEE	PERIGEE	INCL	DRIFT
[illegible]	64 [illegible]	H	[illegible]	[illegible]	80[illegible]	[illegible]	-65.4324	60.2090	34811	34890	2041	48.34	21.1039
[illegible]	64 [illegible]	D	[illegible] 4	[illegible]	80118.8216	[illegible]	-21.2347	-141.3238	14092	33858	2153	67.59	11.6958
[illegible]	64 [illegible]		[illegible] 4 [illegible]	[illegible]	80118.7560	[illegible]	-39.1413	-130.0510	26952	34029	2042	67.37	12.0234
83545	[illegible]	A	[illegible]	[illegible]	79203.7403	280.3	-2.3850	95.7989	17967	18139	17956	2.13	12.0249
[illegible]	77 14	A	[illegible]	JAPAN	80 19.3027	103.7	-0.4020	122.8930	19324	19331	19317	0.17	0.0185
[illegible]	78 [illegible]	A	[illegible]-2	NASA	80 96.3949	22.6	0.2141	5.5215	19390	19398	19318	0.41	-1.0137
[illegible]	77 [illegible]	A	[illegible]	JAPAN	80105.0474	14.0	-0.8970	140.3289	19323	19327	19321	0.90	0.0187
[illegible]	77 [illegible]	A	[illegible]-B	NASA	80115.7120	2.3	0.2177	-110.1940	19324	19327	19323	0.91	-0.0055
[illegible]	78 [illegible]	A	[illegible]-C	NASA	80116.7809	2.2	-0.0154	-135.0284	19327	19328	19320	0.09	-0.0016
11199	79[illegible]	A	[illegible]	USSR	79273.3935	213.6	6.6146	120.0562	20703	25948	12693	10.95	0.0861
11440	79 [illegible]	A	[illegible] 2	USSR	80114.4516	4.5	-0.1943	-14.1944	19319	19331	19317	0.21	0.0098
11648	79[illegible]	A	[illegible] 3	USSR	80106.2868	12.7	-0.0568	53.1007	19290	19350	19287	0.58	-0.0006
11694	79[illegible]	E	[illegible] 3 R/B	NORAD	80112.9980	5.0	0.4936	116.1430	19543	19651	19535	0.58	-5.7190
83582	TEST	A	[illegible] 1-9 R/B	NORAD	80117.7123	1.5	7.3956	-51.4358	18349	18658	18194	10.01	22.5275
83597	TEST	A	[illegible] 17-19 R/B	NORAD	80117.2044	1.8	-0.6410	-158.7033	18097	18150	17972	2.64	32.0180
83545			[illegible] 20-27 R/B	NORAD	80 93.8433	25.2	-4.2906	24.4257	18893	18928	18196	9.68	19.1737
[illegible]	75 42	A	INTELSAT IV F1	COMSAT	80116.4580	2.5	-0.0272	-18.5261	19325	19326	19324	0.08	-0.0120
[illegible]	74 [illegible]	A	INTELSAT IV F8	COMSAT	80115.9253	3.1	-0.0501	173.8352	19324	19338	19319	0.10	0.0017
[illegible]	69 2[illegible]	A	INTELSAT 3-F1	NORAD	79 49.8250	434.2	6.9489	-147.2232	19389	19396	19265	11.41	-0.0223
03674	69 11	A	INTELSAT 3 F3	COMSAT	80 14.6525	104.3	-5.4449	71.9266	19313	19338	19309	6.50	0.0194
83519	TEST	A	INTELSAT 3 F4	NORAD	80 85.8722	33.1	-6.0107	145.8598	19579	19875	18181	9.20	7.1688
[illegible]	71 [illegible]	A	INTELSAT 4 F2	COMSAT	80116.8306	2.4	1.5933	-1.6500	19328	19329	19317	2.30	0.0382
[illegible]	71 [illegible]	A	INTELSAT 4 F3	COMSAT	80116.4658	2.5	-0.0117	-21.3250	19329	19335	19321	0.02	-0.0205
[illegible]	72 [illegible]	A	INTELSAT 4 F4	COMSAT	80116.9088	2.1	-0.2569	178.8018	19319	19338	19319	0.29	-0.0010
[illegible]	72 4[illegible]	A	INTELSAT 4 F5	COMSAT	80112.2577	6.7	0.0868	57.9165	19327	19329	19320	0.09	0.0140
[illegible]	73 58	A	INTELSAT 4-F7	COMSAT	80112.2619	6.7	0.0932	56.3892	19321	19326	19322	0.25	0.0144
[illegible]	75 [illegible]	A	INTELSAT 4AF-1	COMSAT	80117.4717	1.5	0.0434	-24.4603	19331	19331	19318	0.08	-0.0020
[illegible]	76 [illegible]	A	INTELSAT 4AF-2	COMSAT	80116.4550	2.5	-0.0250	-27.5265	19327	19327	19323	0.01	-0.0115
[illegible]	76 [illegible]	A	INTELSAT 4AF-3	COMSAT	80112.2565	6.7	0.0282	63.5251	19326	19329	19321	0.15	0.0164

SYNCHRONOUS CATALOG FOR DATE=80117, (28 APR 80)

					EPOCH	DT	LATITUDE	LONGITUDE	HEIGHT	APOGEE	PERIGEE	INCL	DRIFT
10024	77 41	A	INTELSAT 4AF-4	COMSAT	80113.5107	5.5	-0.0101	-34.5415	19326	19327	19323	0.01	[illegible]
10778	78 35	A	INTELSAT 4AF-6	COMSAT	80112.2432	5.8	0.0006	63.0271	19325	19326	19323	0.01	[illegible]
10637	78 12	A	IUE	NASA	80116.0340	5.0	-4.9924	-34.9405	16858	24451	13980	28.24	0.8941
03431	69 5	D	LES 6	LCN LAB	80112.8313	5.2	5.5936	-107.5217	19323	19352	19318	6.19	-0.2454
83522	DESTT	A	LES 6 R/B	NORAD	80106.5504	12.4	-4.6950	58.0171	19224	19328	18966	5.98	4.5600
08746	76 23	A	LES-8	LCN LAB	80117.8033	1.3	22.8808	-105.2596	19318	19328	19318	25.28	0.0384
08751	76 23	F	LES-8+9/SOL-114,8 R/B 2	NORAD	80117.7607	1.2	24.7574	-146.6339	19943	19956	19302	25.40	-7.2334
08747	76 23	B	LES-9	LCN LAB	80115.6572	5.3	12.9637	-93.4104	19325	19338	19317	25.24	0.0219
08697	76 17	A	MARISAT 1	NASA	80114.4542	4.5	0.8983	-15.2295	19319	19331	19319	0.91	-0.0220
08882	76 53	A	MARISAT 2	NASA	80115.9181	3.1	-0.2625	176.4200	19320	19320	19320	0.35	-0.0001
09478	76101	A	MARISAT-3	NASA	80112.1136	5.9	-0.8803	72.6588	19321	19331	19319	1.47	-0.0102
10489	77108	A	METEOSAT	ESA	80106.4348	12.6	0.4996	0.7830	19367	19358	19262	0.52	0.0799
07392	74 67	A	MOLNIYA 1-S	NORAD	74210.1785	2097.8	-2.5568	154.7009	19349	19355	19355	0.07	-0.2358
08808	76 35	A	NATO IIIA	NATO	80 85.8129	31.8	-0.4582	-18.3801	19317	19334	19316	1.10	-0.0160
04353	70 21	A	NATO 1	NATO	80100.9276	16.1	3.2550	-105.5989	19333	19337	19313	4.98	-0.0019
04902	71-09	A	NATO 2	NATO	80 24.1070	94.9	-3.6820	161.3117	19327	19328	19091	5.09	2.7494
09785	77 5	A	NATO 3-B	NATO	80112.3789	5.6	-0.7719	-80.6305	19469	20259	18380	1.00	0.0117
11115	78105	A	NATO-IIIC	NATO	80113.3848	5.6	-2.4855	-50.0771	19310	19341	19310	3.30	-0.0163
05851	72-10	A	DPS 1570	SCF	80113.0195	4.0	-0.2386	-162.9698	19320	19350	19284	6.02	-0.1988
83524	DESTT	A	DPS 1570 R/B (2)	NORAD	80117.8632	1.1	4.7298	-108.7643	19123	19436	19121	5.98	1.4518
09718	76 53	A	DPS 2112	SCF	80115.5144	1.2	2.6843	-69.3091	19320	19339	19313	2.87	-0.0379
09918	76 53	C	DPS 2112 R/B (2)	NORAD	80111.9378	7.1	1.7071	-102.0188	19252	19311	19250	2.89	1.0546
09833	77 7	A	DPS 3151	SCF	80111.4482	7.6	-1.0357	69.2572	19331	19331	19321	2.37	-0.0348
09835	77 7	C	DPS 3151 R/B (2)	NORAD	80118.8166	1.2	2.1587	-70.0822	19354	19356	19275	2.38	0.0927
04492	75118	A	DPS 3145	NORAD	80112.4465	5.4	2.1499	-3.1395	19333	19358	19225	3.31	0.4494
05516	[illegible]	[illegible]	DPS 3145 R/B (2)	NORAD	80116.3270	2.7	-3.0809	103.9075	19299	19359	19218	3.37	0.8548
05204	71 32	A	DPS 3811	SCF	80109.3657	10.6	-5.8504	74.4466	19328	19338	19319	6.83	-0.0074
83518	DESTT	A	DPS 3811 R/B (2)	NORAD	80 77.5537	41.4	-5.2824	61.9949	19548	19573	19028	7.08	0.8488
04570	[illegible]	A	DPS 5940	NORAD	80113.0211	5.0	8.1534	-78.8020	18699	19550	13877	10.34	71.7211

SATELLITE	DESIGNATION		NAME	SOURCE	EPOCH	AGE	LATITUDE	LONGITUDE	HEIGHT	APOGEE	PERIGEE	INCL	DRIFT
14452	[illegible]	B	OPS [illegible]	NORAD	80117.9235	1.2	7.5740	2.3035	14956	19633	13856	10.39	71.8440
05431	72-41	A	OPS A157	SCF	80113.8716	5.1	4.1447	-99.9254	19330	19148	19297	9.30	0.0459
83532	TEST	A	OPS A157 R/B (2)	NORAD	80118.1324	0.9	-3.9843	159.7472	19377	19528	19317	5.29	-2.3294
17549	74 15	A	OPS A391	SCF	80113.3729	5.6	-0.9287	-99.2981	19321	19335	19315	1.17	-0.0143
11393	79 39	A	OPS 4392	SCF	80102.0591	16.2	-0.1446	72.3538	19364	19373	19274	2.00	0.0302
11459	8- 4	A	OPS A393	SCF	80116.3551	2.6	-2.0327	-22.6881	19314	19334	19298	2.54	-0.0367
11337	79 53	A	OPS 7484	SCF	80114.5681	4.4	0.4476	-132.7076	19323	19329	19316	1.29	0.0381
11435	79 53	B	OPS 7484 R/B (2)	NORAD	80112.1386	5.9	-1.1945	2.9221	19409	19531	19377	1.29	-3.0588
02693	67 3	F	OPS 9326 (IDCSP 13)	NORAD	79229.2782	254.7	-9.2656	102.9498	18378	18330	18135	9.24	26.0717
03290	68 53	G	OPS 9347 (IDSCS 26)	NORAD	78 65.0000	782.0	6.9193	-40.0668	18307	18475	18251	7.51	24.3860
05557	71 95	A	OPS 9431	NORAD	80117.8876	1.1	7.7309	-107.4065	19338	19338	19308	4.14	0.0343
83515	TEST	A	OPS 9431+2 R/B 2	NORAD	80112.4995	5.8	3.8376	-31.4969	19497	20138	19465	4.33	-11.0274
05598	71 95	B	OPS 9432	NORAD	80118.0799	0.9	-1.8966	-177.3390	19330	19337	19323	4.02	-0.1363
05973	73109	A	OPS 9433	SCF	80116.8918	2.1	1.6671	-90.2343	19345	19347	19326	2.59	-0.2835
83540	TEST		OPS 9433/9434 RB	NORAD	80114.1032	4.9	-2.8961	105.0999	20794	20837	19495	2.98	-18.3977
06974	73109	B	OPS 9434	SCF	80104.5130	14.5	-0.4309	98.6491	19297	19337	19297	2.68	-0.0634
10000	77 34	A	OPS 9437	SCF	80114.1416	4.9	0.4156	104.6727	19321	19339	19171	0.61	1.4306
10002	77 34	C	OPS 9437/9438 R/B (2)	NORAD	80118.8301	0.4	-0.2238	-66.8198	19457	20911	19321	0.44	-16.0798
10001	77 34	B	OPS 9438	SCF	80113.7882	5.2	-0.3974	-143.8296	19331	19434	19331	0.47	-1.0656
11144	78113	A	OPS 9441	SCF	80116.5044	2.5	-0.0862	-135.0192	19326	19326	19321	1.47	0.0245
11147	78113	C	OPS 9441+2 R/B(2)	NORAD	79257.0281	227.0	0.7896	72.1443	18243	19109	17466	1.69	26.1407
11145	78113	B	OPS 9442	SCF	80117.6414	1.4	1.1017	175.4629	19325	19329	19323	1.48	-0.0059
11671	79 98	A	OPS 9443	SCF	80113.2375	5.8	-2.0494	-12.3631	19326	19330	19318	2.19	0.0027
11673	79 98	C	OPS 9443/9444 RB	NORAD	80118.2659	0.7	-1.9929	-46.6962	19822	20879	19336	2.04	-17.8546
11672	79 98	B	OPS 9444	SCF	80108.0290	10.0	0.3921	65.6391	19323	19326	19324	2.09	-0.0083
13955	79 44	A	[illegible]	ESA	80112.3901	6.6	0.0117	9.9824	19348	19372	19277	0.03	-0.0060
83530	68 81	A	[illegible]	NORAD	79241.0055	242.0	4.2673	-53.3007	19900	20078	18229	5.00	4.1244
09009	76 65	A	PA APAFA	INTOLES	80113.3035	5.7	-6.3146	80.9985	19377	19370	19324	6.68	-0.6433
09842	77 19	A	PA APA-B [illegible]	INTOLES	80116.4187	2.4	-2.5142	74.4051	21979	22039	16613	3.59	-0.2220

SYNCHRONOUS CATALOG FOR DATE=80119, (28 APR 80)

					EPOCH	RT	LATITUDE	LONGITUDE	HEIGHT	APOGEE	PERIGEE	INCL	DRIFT
89515			POSSIBLE 9503 FRAG-1	AEROSP	79243.4359	249.9	-1.2403	75.6732	19410	19458	19196	1.73	-0.0644
02416	76 92	A	RADUGA (2)	USSR	79211.0742	272.9	2.2127	-107.5282	14529	24133	14463	2.37	0.4283
11558	79123	F	RADUGA 1 R/B	NORAD	80110.7301	5.3	2.7167	-31.1658	19261	19322	19261	2.93	0.7824
11570	77 71	F	RADUGA 3 RB	NORAD	80113.8170	5.2	0.6949	-107.0516	19685	19755	19682	1.68	-9.1259
83535	78 73		RADUGA 4 R/B	NORAD	80113.5493	5.5	0.3621	-101.7443	19729	19779	19708	0.88	-9.7362
11736	80 15	A	RADUGA 6	USSR	80113.3184	5.7	-0.1512	34.6614	19297	19371	19277	0.29	0.0199
11728	80 15	D	RADUGA 6 RB	NORAD	80115.8642	5.1	0.3190	166.0661	19735	19758	19758	0.31	-9.4406
10159	77 71	A	RADUGA-3	USSR	80 49.6648	69.3	-0.3464	39.3703	19400	19419	19228	1.19	0.0202
13957	78 73	A	RADUGA-4	USSR	80 63.4846	55.5	0.5628	39.8280	19358	19378	19248	1.03	0.0293
11343	79 35	A	RADUGA-5	USSR	80108.1967	10.8	-0.0805	63.2303	19330	19338	19323	0.28	-0.0081
09476	75117	A	RCA-A	RCA	79232.4391	251.6	-0.3912	-77.3870	19321	19326	19245	0.83	0.1983
09774	76 29	A	RCA-B	RCA	80116.7364	2.3	-0.0173	-118.9841	19323	19329	19322	0.02	-0.0019
11236	79 7	A	SCATHA	SCF	80111.3605	7.6	-6.5038	-26.0661	18064	23358	14845	6.87	5.6075
10294	77 80	A	SIRIO	ITALY	79347.3272	135.7	-0.6859	-170.8353	19960	20006	18674	1.59	-0.1761
04250	69101	A	SKYNET A	GR BRIT	80104.8846	14.1	4.7816	-105.9416	19554	19571	19057	5.78	0.0100
07547	74 94	A	SKYNET 2B	GR BRIT	80 68.6407	50.4	-0.4633	42.0761	19077	19552	19076	1.71	0.3921
07298	74 33	A	SMS-A	NASA	80111.0546	7.9	-1.2462	-139.8118	19318	19358	19316	4.60	-0.2109
07648	75 11	A	SMS-B	NASA	80116.6131	2.4	0.3948	-74.5336	19374	19358	19270	0.59	-0.0072
08366	75100	A	SMS-C(GOES A)	NASA	80100.9650	18.0	0.5559	-88.6989	19436	19438	19191	1.09	-0.0011
07578	74101	A	SYMPHONIE-A	FRANCE	80100.7307	19.3	1.1255	-12.0090	19321	19332	19318	1.23	-0.0103
08192	75 77	A	SYMPHONIE-B	FRANCE	80100.7094	19.3	1.4801	-11.5187	19318	19335	19298	1.74	-0.0058
83595			UNK POS RADUGA 1	NORAD	80108.4095	10.6	-0.7764	84.0659	19317	19338	19314	2.18	-0.0279
83598			UNK POS USSR RB	NORAD	80 54.6222	64.4	-2.8813	73.5285	18981	20578	18559	4.49	0.1694
83597			UNK POS 4250,4253,4902	NORAD	80 63.1738	55.8	-0.9270	-113.4702	19271	19329	19271	3.73	-0.1844
83514	87? ?	A	UNK POS 4250,4253,4902	NORAD	80118.2399	2.1	0.9903	-113.7416	19248	19379	19246	2.51	-0.1596
83293			UNKNOWN	NORAD	80105.4203	13.6	-0.0455	10.1236	19503	19539	19083	0.08	0.0342
83503			UNKNOWN	NORAD	80 11.1216	107.9	-1.9111	84.0293	19243	19473	19095	2.67	1.4497
83518	TEST?	A	UNKNOWN	NORAD	79242.4416	241.4	-6.5988	64.4005	20436	20478	18989	7.79	-9.9164
83539			UNKNOWN	NORAD	80112.5541	6.4	0.3937	76.1945	19128	19949	19142	1.67	0.0496

SYNCHRONOUS CATALOG FOR DATE=80119, (28 APR 80)				EPOCH	DT	LATITUDE	LONGITUDE	HEIGHT	APOGEE	PERIGEE	INCL	DRIFT
83550		UNKNOWN	NORAD	80113.8740	5.1	1.8650	-86.1043	19190	19549	19167	2.48	-0.0774
83553		UNKNOWN	NORAD	80113.7904	5.2	0.0054	-134.8504	19238	19414	19234	0.10	0.0193
83573	TESTT A	UNKNOWN [illegible]	NORAD	80 49.8516	69.3	-1.3320	81.1239	19301	19672	18962	2.30	0.1858
83591	TESTT A	UNKNOWN [illegible]	NORAD	79194.2341	289.7	-0.0833	-138.8344	20908	21358	17607	1.15	-3.7109
07250	74 22 A	WESTAR A	WEST UN	80116.8812	2.3	-0.0890	-99.0691	19325	19328	19322	0.04	-0.0127
11494	79 72 A	WESTAR C	WEST UN	80116.6587	2.3	-0.0845	-90.9486	19326	19328	19321	0.02	-0.0098
07456	74 75 A	WESTAR-B	WEST UN	80118.7435	0.3	0.0946	-123.4959	19324	19329	19322	0.03	-0.0023
83923		SILVER FOX 4 DM	NORAD	80 28.4923	91.1	0.4515	116.0599	19540	19606	19531	0.79	-5.9327
83691		83691	NORAD	80117.8500	1.1	0.1614	-171.6690	19731	19739	19723	0.21	-9.9735
83743		83743	NORAD	80118.9242	0.1	0.6992	-104.2659	19388	19408	19324	1.51	-0.0914

Notes:

1) Date of the orbit element set (year, day number, fraction of day)

2) Time since epoch of element set (days)

3) Position of object on 28 April 1980 at 0000 Z (deg N, deg E, nmi)

4) Orbital parameters for epoch data (nmi, nmi, deg)

5) Longitude drift rate for epoch date (deg/day East) - Westerly (negating) drift for mean motion n < 1.002738 revolutions/day.

REFERENCES

1. V.A. Chobotov, "On The Probability of Satellite Collisions in Earth Orbits," TOR-0079(4071-07)-1, The Aerospace Corporation, El Segundo, CA June 21, 1979.

2. D.J. Kessler, P.M. Landry, B.G. Cour-Palais, R.E. Taylor, "Collision Avoidance in Space," IEEE Spectrum, June 1980.

3. R.A. Marsh, Private Communication.

4. Revised Table of Earth Satellites, Royal Aircraft Establishment Farnborough, Hants., England, Vol. 2 (1969-1973).

5. W.A. Feess, "Reconstruction of Skynet #2(B) Apogee Burn Performance," TOR-0059(6112-10)-4, The Aerospace Corporation El Segundo, CA, February 1971.

6. L.J. Tedeschi, "Analysis of Doppler Data in Support of the Skynet 2 Failure Investigation," TOR-0059(6112-10)-3, The Aerospace Corporation, El Segundo, CA.

7. G. Wrenn, "Geos 2 in Space Collision?," Nature Vol. 274, 17 August 1978.

8. D.J. Kessler and B.G. Cour-Palais, "Collision Frequency of Artificial Satellites: The Creation of a Debris Belt," J. Geophysical Res., Vol. 83, No. A6, June 1, 1978.

9. W.L. Morgan, "Geosynchronous Satellite Log," COMSAT Technical Review, Vol. 8 No. 1, Spring 1978, pp. 219-237.

10. W.L. Morgan, "Satellite Utilization of the Geostationary Orbit," COMSAT Technical Review, Vol. 6, No. 1, Spring 1976, pp. 195-205.

11. D.H. Martin, Communication Satellites 1958 to 1982," TR-79-078, The Aerospace Corporation, El Segundo, CA, September 10, 1979.

12. Physical Nature and Technical Attributes of the Geostationary Orbit - Study Prepared by the Secretariat of the United Nations, A/AC. 105/203 29 August 1977.

13. E.J. Öpik, Interplanetary Encounters (Close-Range Gravitational Interactions), Elsevier Scientific Publishing Co. New York, 1976.

14. T.R. Gurlitz "Program MINRNG," TOR-0080(5409-49)-1, The Aerospace Corporation, El Segundo, CA, May 7, 1980.

15. Collision Probability of the Apollo Spacecraft with Objects in Earth Orbit, NASA MSC Internal Note No. 67-FM-44, April 10, 1967.

16. M.R. Spiegel, Probability and Statistics, Shaum's Outline Series, McGraw-Hill Book Co., September 1975.

DATE
FILMED

-8